

Supplementary Information

Substituent effects and electron delocalization in five-membered N-heterocycles

Paweł A. Wieczorkiewicz^{1,*}, Tadeusz M. Krygowski², Halina Szatylowicz^{1,*}

¹ Faculty of Chemistry, Warsaw University of Technology, Noakowskiego 3, 00-664 Warsaw, Poland

² Department of Chemistry, University of Warsaw, Pasteura 1, 02-093 Warsaw, Poland

Table of Contents

Computational details

Figure S1. Relations between characteristics of five-membered N-heterocyclic rings and number of cyclically delocalized electrons, $\text{EDDB}_P(\pi)$.

Table S1. Coefficients a (slope) and R^2 of linear correlations between $\text{EDDB}_P(\pi)$ and cSAR(X) presented in Figure 2.

Table S2. Isosurfaces of $\text{EDDB}_P(\pi)$ function (0.02), representing the density of cyclically delocalized π -electrons.

Figure S2. Relationships between $\text{EDDB}_P(\pi)$ and resonance substituent constant R .

Figure S3. Relations between lengths of bonds in the ring and resonance R constants (left column) or the number of cyclically delocalized π -electrons, $\text{EDDB}_P(\pi)$ (right column).

Figure S4. NBO analysis – natural hybrid orbital character of hybrids at ring atoms. Example – C4 substituted pyrazole derivatives (pyraC4).

Table S3. Crystallographic data found for monosubstituted compounds in CCSD.

Figure S5. π -Orbital shapes independent of X substituent type.

Table S4. Isosurfaces of EDDB_{G-P} function (0.02 electrons) – a visual representation of non-cyclic electron delocalization.

Table S5. Values of cSAR(X) for NO_2 , Cl and NH_2 substituents, the number of inductive and resonance interactions between substituent and endocyclic N atoms in each heterocycle and resonance structures associated with resonance effect of substituents.

Table S6. Values of cSAR(X) of NO_2 , Cl and NH_2 substituents in derivatives of selected six-membered heterocycles.

Figure S6. Relations between geometric aromaticity indices and the number of cyclically delocalized electrons from the $\text{EDDB}_P(\pi)$ function.

Figure S7. Non covalent interaction analysis (NCI method). Reduced density gradient isosurfaces ($\text{RDG} = 0.5$), colored according to the value of $\text{sgn}(\lambda_2(r)) \cdot \rho(r)$.

Table S7. Keto, thioketo and imino forms of studied five-membered heterocycles with their $\text{EDDB}_P(\pi)$, cSAR(X), HOMED, CX bond lengths (d_{CX}) and ΔE values (in kcal/mol).

Figure S8. Anisotropy of the induced current density (AICD) plots and EDDB_P isosurfaces (0.02) for enol and keto forms of substituted imidazole and pyrazole.

Figure S9. Correlation between the number of cyclically delocalized electrons and electron withdrawing properties of $=\text{NH}/=\text{O}/=\text{S}$ groups for all studied heterocycles.

Figure S10. Energies of HOMO, LUMO and the HOMO–LUMO gap ($\Delta H-L$) as a function of cSAR(X).

Table S8. Summary of slopes from Figure S10.

Table S9. Reference bonds lengths (\AA) calculated at revDSD–PBEP86–G3BJ/def2–TZVPP level of theory and values of HOMED normalization constants α .

Table S10. AICD plots (isosurface = 0.03) of selected substituted and unsubstituted systems.

Page

S2-S3

S4

S4

S5-S16

S17

S18-S24

S25

S26

S27

S27-S38

S39

S40

S40

S41-S42

S42

S43

S44

S44-S46

S46

S46

S47-50

Computational details

Geometry optimizations and all electronic structure calculations were performed using DFT with double-hybrid functional at revDSD-PBEP86-G3BJ/def2-TZVPP level of theory^{1,2} (tight convergence criteria, UltraFine grid) in Gaussian 16 C.01 program.³ This functional is one of the most accurate DFT methods as tested in several benchmarks.¹ Vibrational frequencies calculations were performed to confirm that each optimized geometry correspond to the minimum on the potential energy surface. Natural orbital calculations were performed using NBO 7 software.⁴

EDDB is a method which allows a very detailed analysis of electron delocalization directly from the information encoded in the wavefunction. In EDDB the total electron density is decomposed into the densities of electrons localized at atoms (core electrons, lone pairs), localized at chemical bonds, and delocalized between several bonds. The last density is called electron density of delocalized bonds (EDDB), from which the method takes its name. Full theory on how decomposition is performed we refer the readers to the cited articles.⁵⁻⁸

The EDDB can be further decomposed into contributions from different delocalization types. EDDB_G (G - global) contains all delocalized electrons, EDDB_H excludes the contribution from bonds with H atoms, while EDDB_P contains only electrons delocalized in cyclic Kekulean pathway (excluding cross-ring delocalization associated in benzene with Dewar forms). Each of the delocalization types can be quantitatively analyzed in terms of contributions from electrons of σ , π and other orbital symmetries. Hence, in this paper, EDDB_p(π) are the cyclically delocalized π electrons. The delocalized electron density grids can be visualized in the form of isosurfaces and subtracted from each other. For example, EDDB_{G-P} = EDDB_G – EDDB_P function is the global electron density minus the cyclically delocalized electron density, in other words, it is a density of non-cyclically delocalized electrons. All EDDB calculations were performed using the density matrices in the NBO basis. EDDB grids were generated in cubegen subprogram available within Gaussian 16 C.01.

HOMA^{9,10} and HOMED^{11,12} geometric aromaticity indices were calculated from Equation 1:

$$\text{HOMA, HOMED} = 1 - \frac{1}{n} \sum_j^n \alpha_j (d_{o,j} - d_j)^2 \quad (1)$$

where n is the number of bonds in considered fragment, α_j is the normalization constant for j bond, for HOMA tabularized (but can also be calculated for specific computational level, Equation 2).

$$\alpha_j = 2\{(d_o - d_s)^2 + (d_o - d_d)^2\}^{-1} \quad (2)$$

For HOMED, if the number of bonds considered is even, Equation 1 is also used. However, if the fragment has odd number of bonds, α_j in HOMED is calculated from Equations 3 or 4:

for a system with i double bonds and $i+1$ single bonds:

$$\alpha_j = (2i + 1) \cdot \{(i + 1)(d_o - d_s)^2 + i(d_o - d_d)^2\}^{-1} \quad (3)$$

for a system with $i+1$ double bonds and i single bonds:

$$\alpha_j = (2i + 1) \cdot \{i(d_o - d_s)^2 + (i + 1)(d_o - d_d)^2\}^{-1} \quad (4)$$

In this paper HOMA was calculated using standard parameters,¹⁰ while HOMED was parametrized at revDSD-PBEP86-G3BJ/def2-TZVPP level of theory, using reference systems proposed by Raczyńska.¹¹ The reference

bond lengths are provided in the Table S9. Calculation of HOMA and HOMED values, as well as EDDB grid subtraction was performed in Multiwfn program.¹³

Anisotropy of the induced current density (AICD)¹⁴ maps were generated using Gaussian and AICD 3.03 program at B3LYP/6-311+G(d,p), NMR=CSGT, with contribution of all orbitals.

Electron donating and withdrawing properties were assessed using the cSAR method. cSAR of substituent X is calculated from Equation 5:

$$\text{cSAR}(X) = q(X) + q(ipso) \quad (5)$$

where $q(X)$ is the sum of charges at all atoms of X, and $q(ipso)$ is the charge at the *ipso* atom of the substituted system, the atom to which X is attached. In this paper, Hirshfeld atomic charges were used.¹⁵

References

- 1 G. Santra, N. Sylvetsky and J. M. L. Martin, *J. Phys. Chem. A*, 2019, **123**, 5129–5143.
- 2 F. Weigend and R. Ahlrichs, *Phys. Chem. Chem. Phys.*, 2005, **7**, 3297.
- 3 M. J. Frisch, G. W. Trucks, H. B. Schlegel, G. E. Scuseria, M. A. Robb, J. R. Cheeseman, G. Scalmani, V. Barone, G. A. Petersson, H. Nakatsuji, X. Li, M. Caricato, A. V. Marenich, J. Bloino, B. G. Janesko, R. Gomperts, B. Mennucci, H. P. Hratchian, J. V. Ortiz, A. F. Izmaylov, J. L. Sonnenberg, Williams, F. Ding, F. Lipparini, F. Egidi, J. Goings, B. Peng, A. Petrone, T. Henderson, D. Ranasinghe, V. G. Zakrzewski, J. Gao, N. Rega, G. Zheng, W. Liang, M. Hada, M. Ehara, K. Toyota, R. Fukuda, J. Hasegawa, M. Ishida, T. Nakajima, Y. Honda, O. Kitao, H. Nakai, T. Vreven, K. Throssell, J. A. Montgomery Jr., J. E. Peralta, F. Ogliaro, M. J. Bearpark, J. J. Heyd, E. N. Brothers, K. N. Kudin, V. N. Staroverov, T. A. Keith, R. Kobayashi, J. Normand, K. Raghavachari, A. P. Rendell, J. C. Burant, S. S. Iyengar, J. Tomasi, M. Cossi, J. M. Millam, M. Klene, C. Adamo, R. Cammi, J. W. Ochterski, R. L. Martin, K. Morokuma, O. Farkas, J. B. Foresman and D. J. Fox, Gaussian 16 Rev. C.01 2016.
- 4 Glendening, E. D., Badenhoop, J. K., Reed, A. E., Carpenter, J. E., Bohmann, J. A., Morales, C. M., Karafiloglou, P, Landis, C. R., and Weinhold, F., NBO 7.0 Theoretical Chemistry Institute, University of Wisconsin, Madison 2018.
- 5 D. W. Szczepanik, M. Andrzejak, K. Dyduch, E. Żak, M. Makowski, G. Mazur and J. Mrozek, *Phys. Chem. Chem. Phys.*, 2014, **16**, 20514–20523.
- 6 D. W. Szczepanik, *Comput. Theor. Chem.*, 2016, **1080**, 33–37.
- 7 D. W. Szczepanik, M. Andrzejak, J. Dominikowska, B. Pawełek, T. M. Krygowski, H. Szatylowicz and M. Solà, *Phys. Chem. Chem. Phys.*, 2017, **19**, 28970–28981.
- 8 D. W. Szczepanik and M. Solà, in *Aromaticity*, Elsevier, 2021, pp. 259–284.
- 9 J. Kruszewski and T. M. Krygowski, *Tetrahedron Lett.*, 1972, **13**, 3839–3842.
- 10 T. M. Krygowski, *J. Chem. Inf. Comput. Sci.*, 1993, **33**, 70–78.
- 11 E. Raczyńska, *Symmetry*, 2019, **11**, 146.
- 12 E. D. Raczyńska, M. Hallman, K. Kolczyńska and T. M. Stępniewski, *Symmetry*, 2010, **2**, 1485–1509.
- 13 T. Lu and F. Chen, *J Comput. Chem.*, 2012, **33**, 580–592.
- 14 Geuenich, D.; Hess, K.; Köhler, F.; Herges, R. *Chem. Rev.* **2005**, *105* (10), 3758–3772
- 15 F. L. Hirshfeld, *Theoret. Chim. Acta*, 1977, **44**, 129–138.

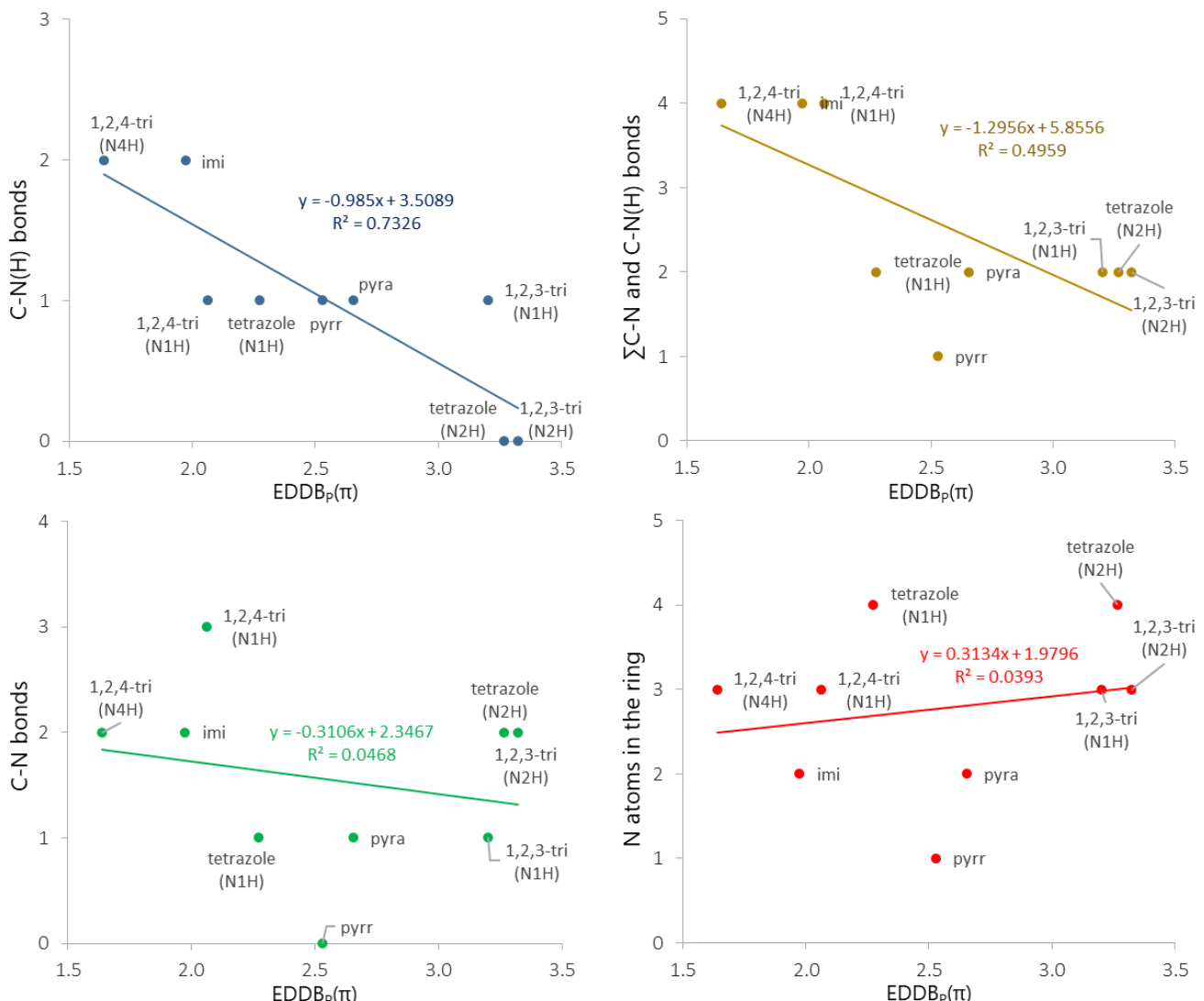
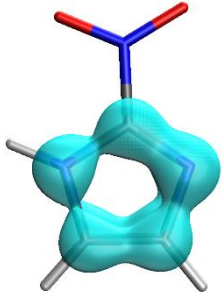
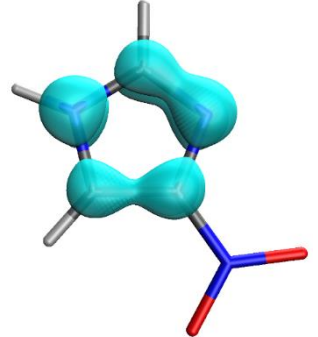
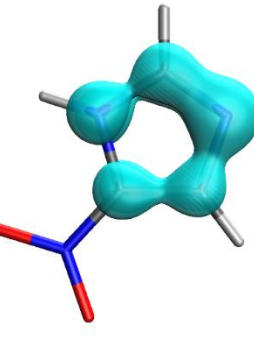
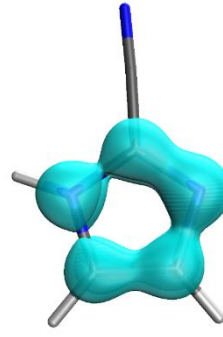
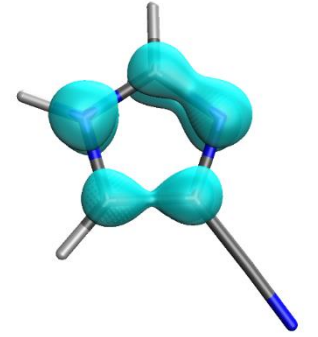
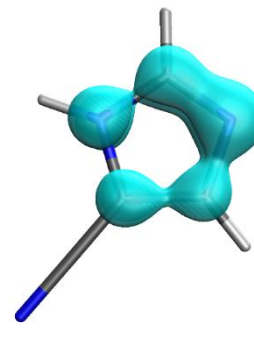
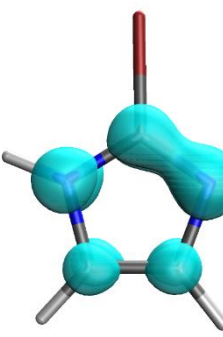
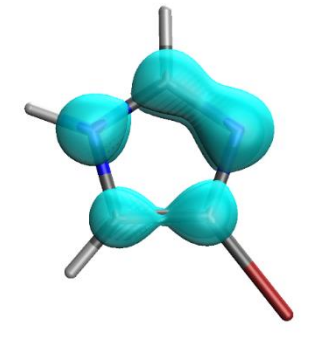
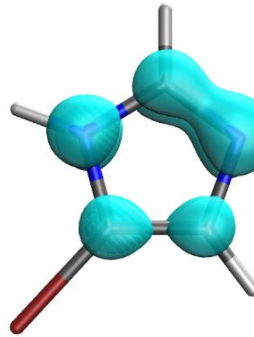
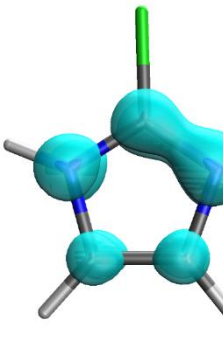
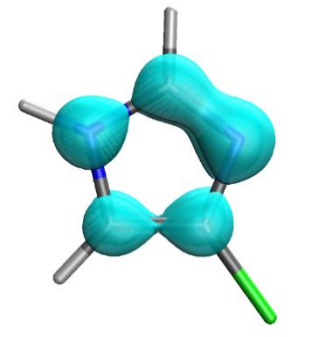
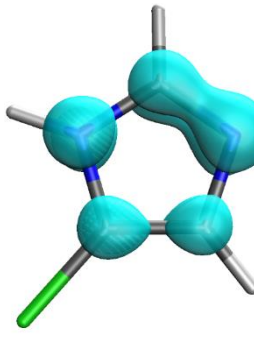


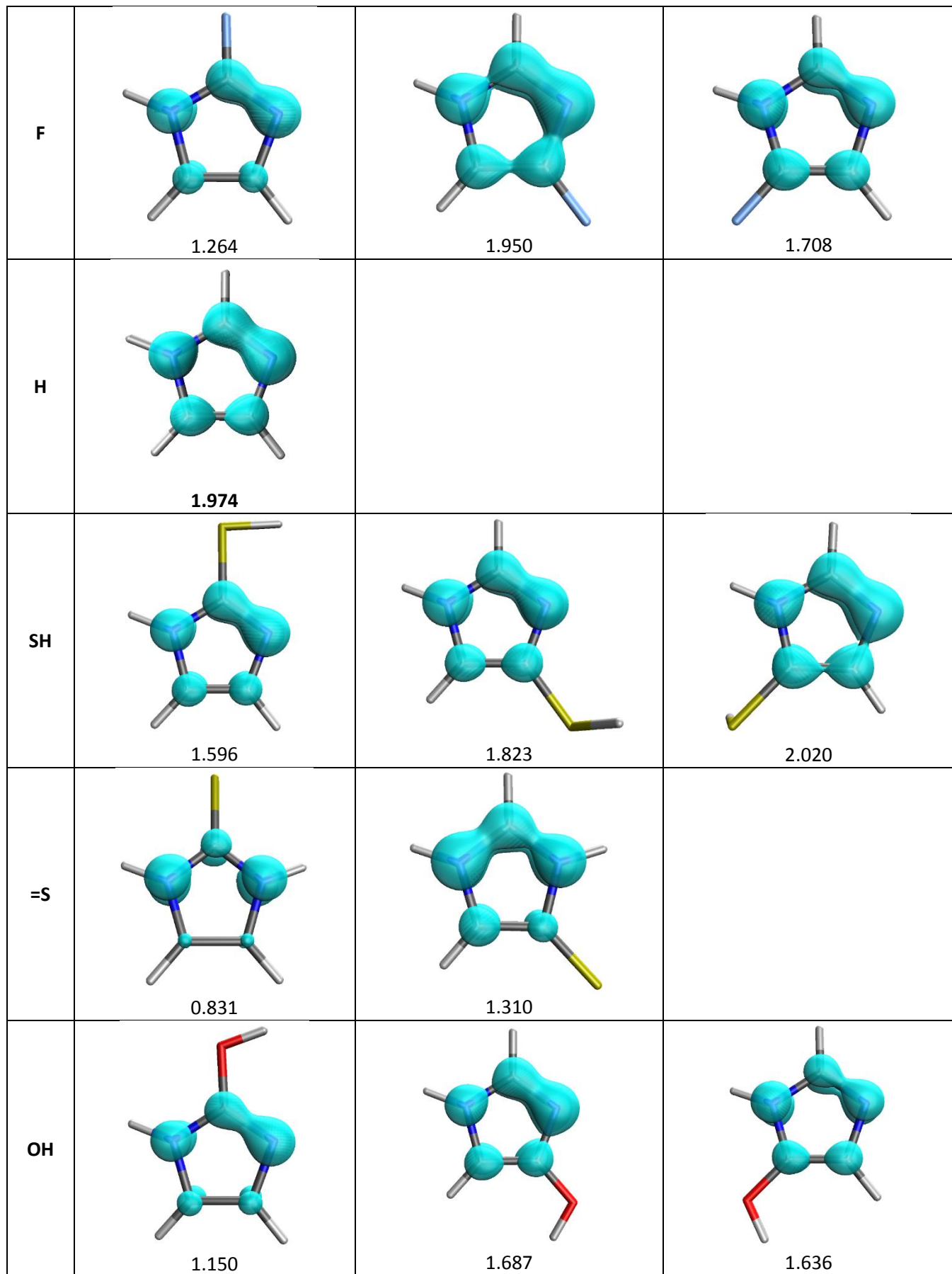
Figure S1. Relations between characteristics of five-membered N-heterocyclic rings and number of cyclically delocalized electrons, EDDB_P(π).

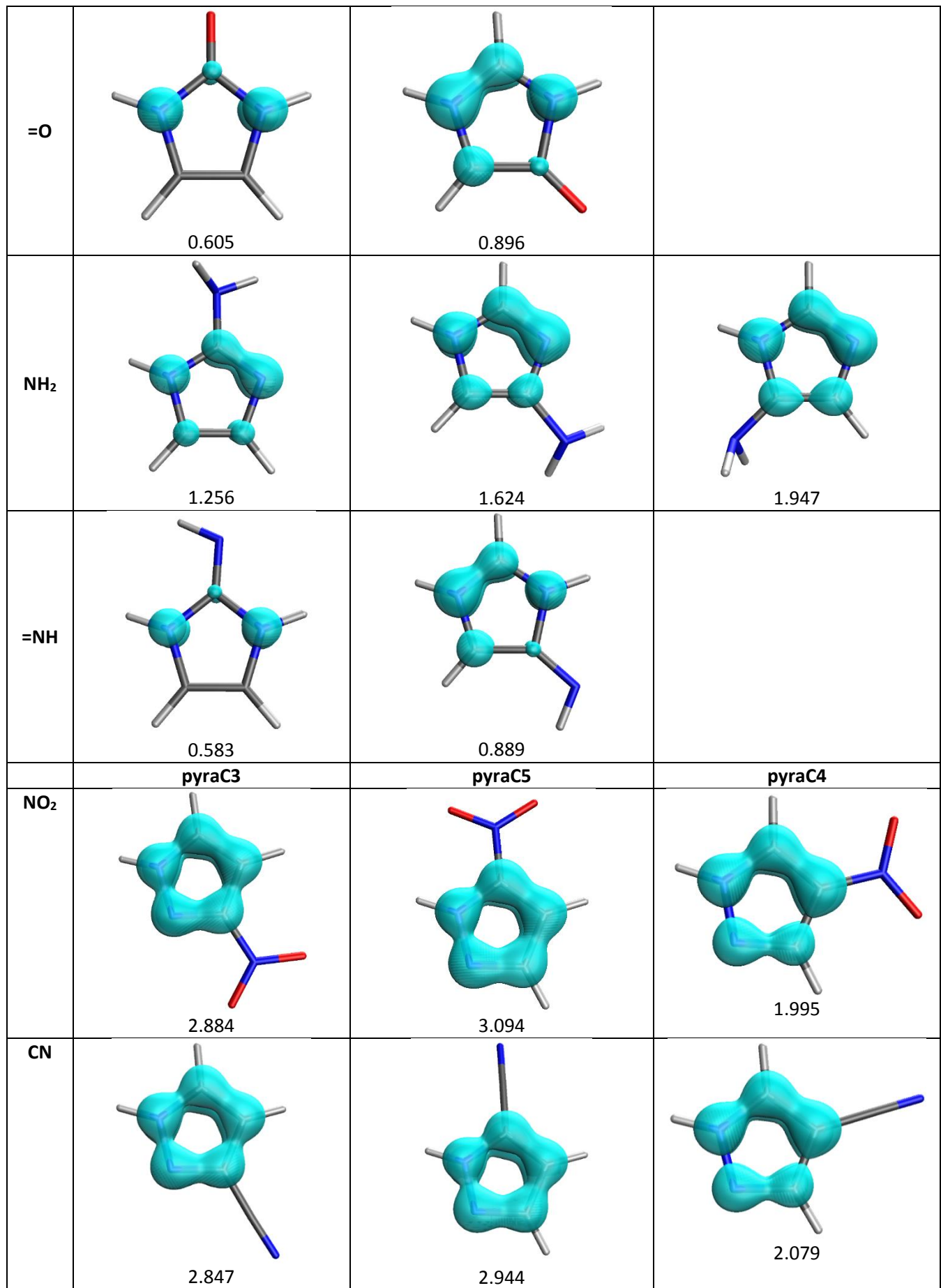
Table S1. Coefficients a (slope) and R^2 of linear correlations EDDB_P(π) vs cSAR(X) presented in Figure 2.

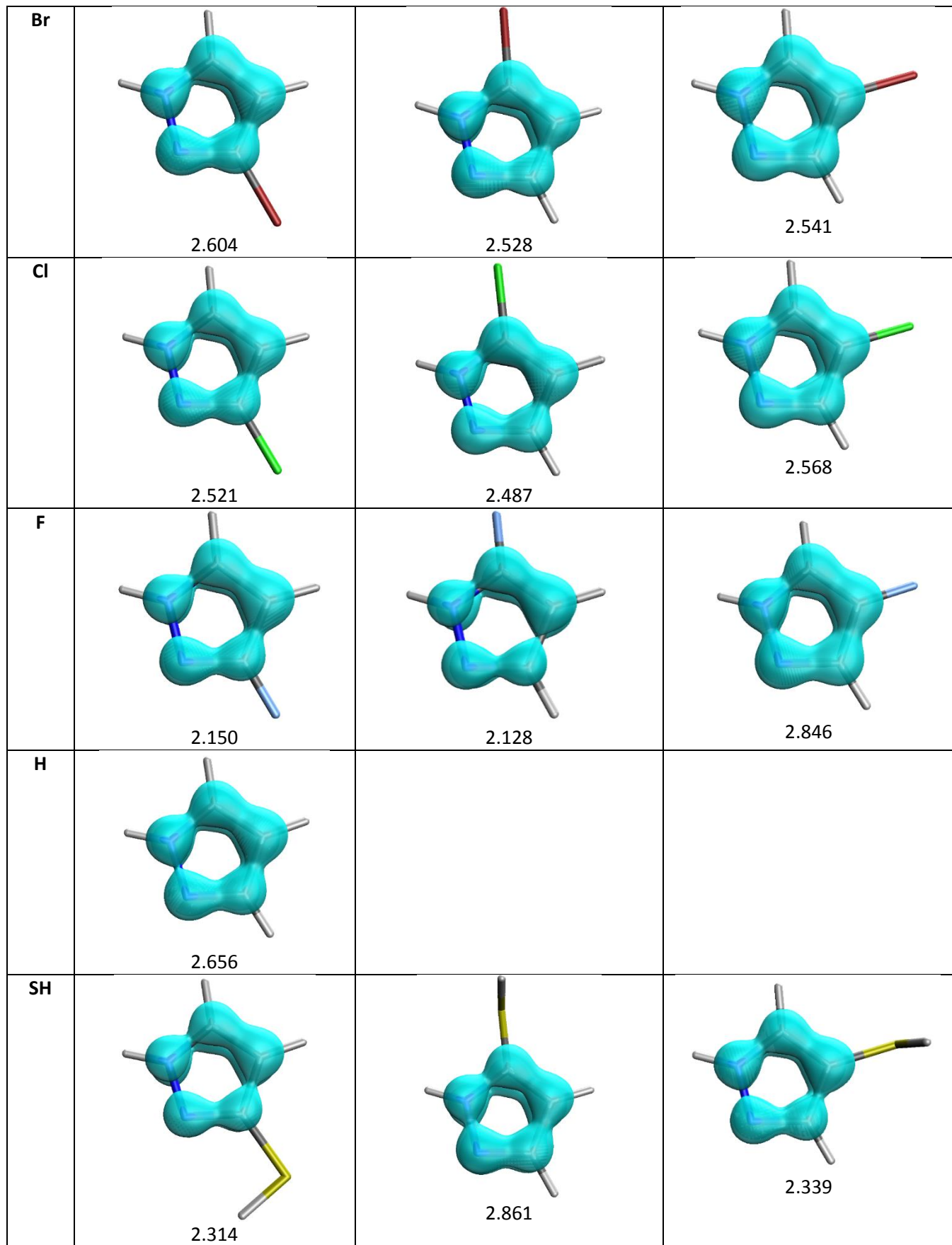
	a	R^2
imiC2	-6.865	0.919
1,2,4-triC3 (N1H)	-5.014	0.872
pyraC3	-4.962	0.902
pyraC5	-4.252	0.785
1,2,4-triC5	-3.844	0.882
1,2,4-triC3 (N4H)	-3.703	0.926
pyrrC2	-2.621	0.448
1,2,3-triC5	-2.421	0.768
1,2,3-triC4 (N2H)	-2.383	0.290
imiC5	-2.070	0.724
imiC4	-2.018	0.781
pyrrC3	0.065	0.001
1,2,3-triC4 (N1H)	0.523	0.081
pyraC4	3.751	0.842

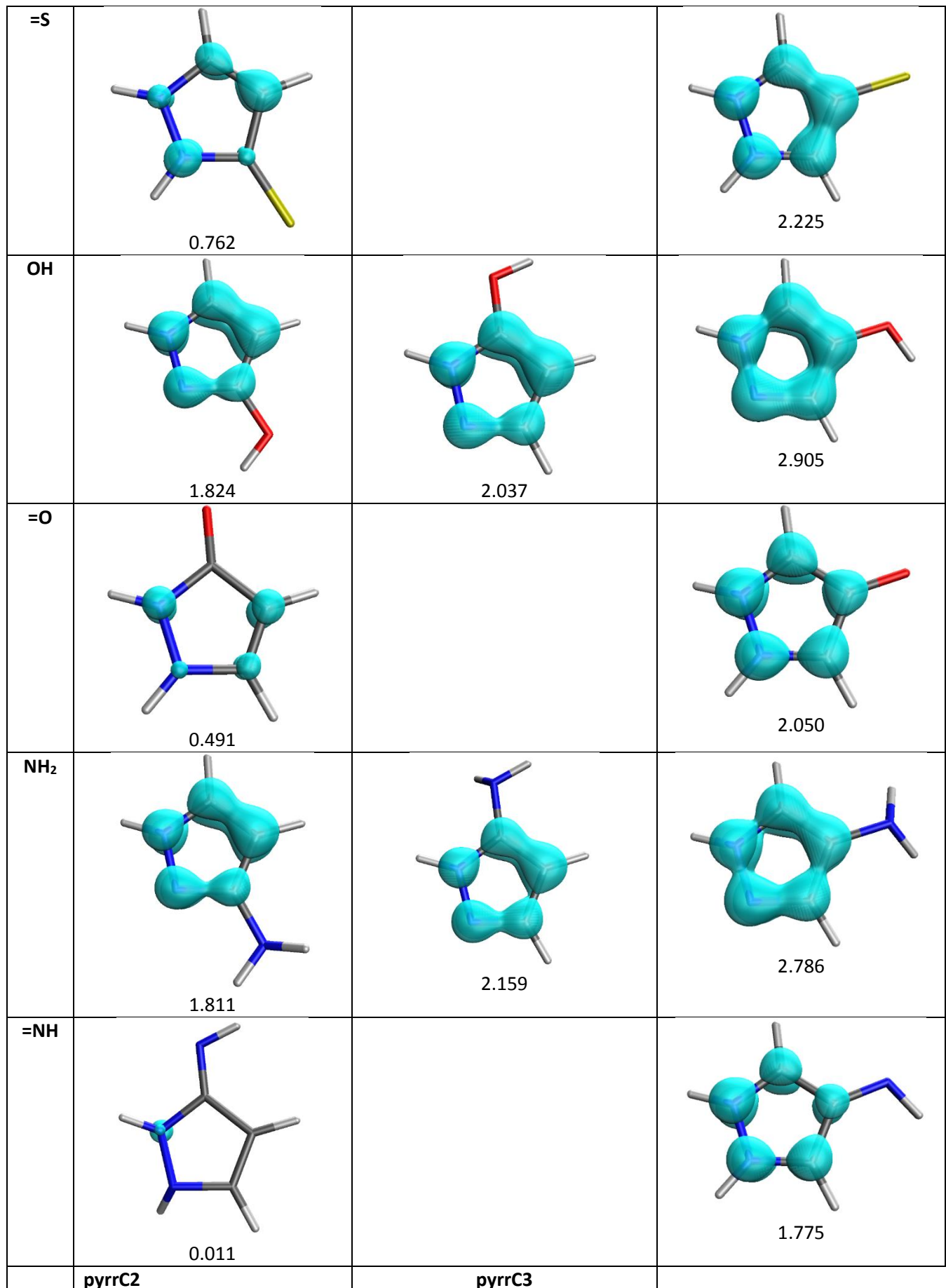
Table S2. Isosurfaces of $\text{EDDB}_\text{P}(\pi)$ function (0.02), representing the density of cyclically delocalized π -electrons.

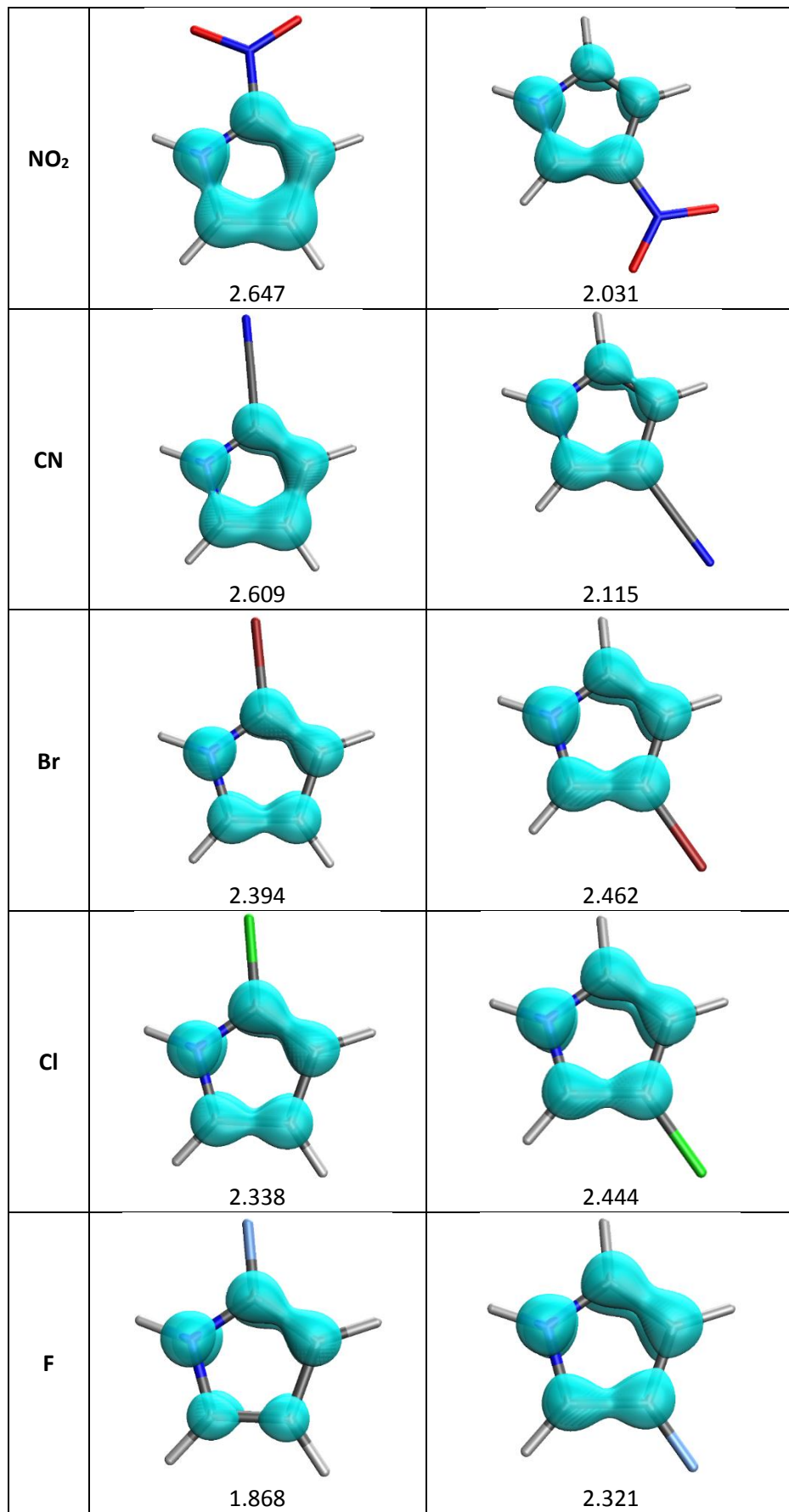
X	imiC2	imiC4	imiC5
NO_2	 2.701	 2.147	 2.257
CN	 2.625	 2.054	 2.145
Br	 1.762	 2.056	 1.886
Cl	 1.708	 2.048	 1.868

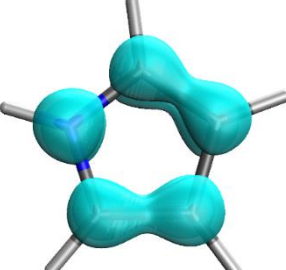
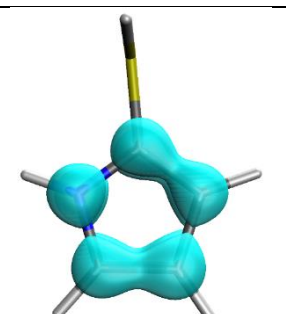
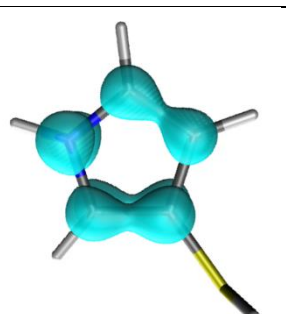
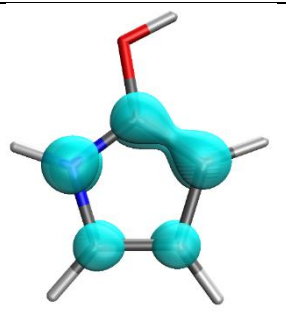
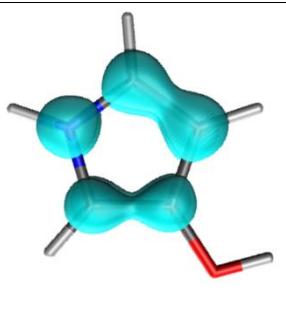
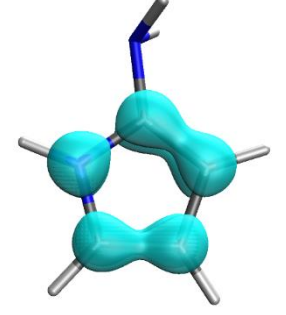
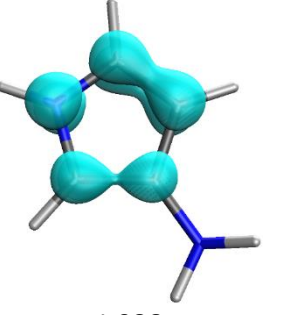
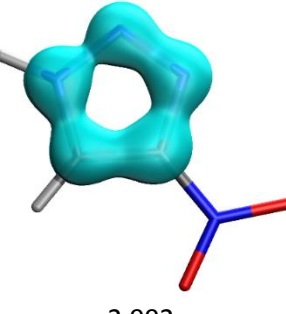
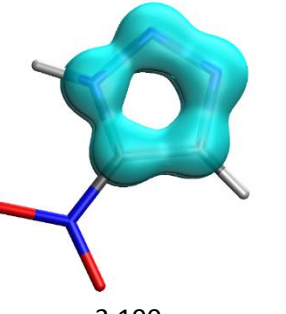
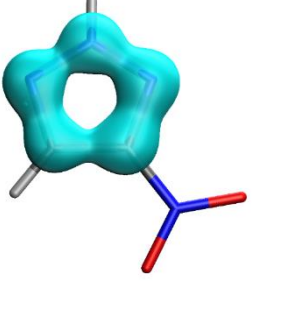


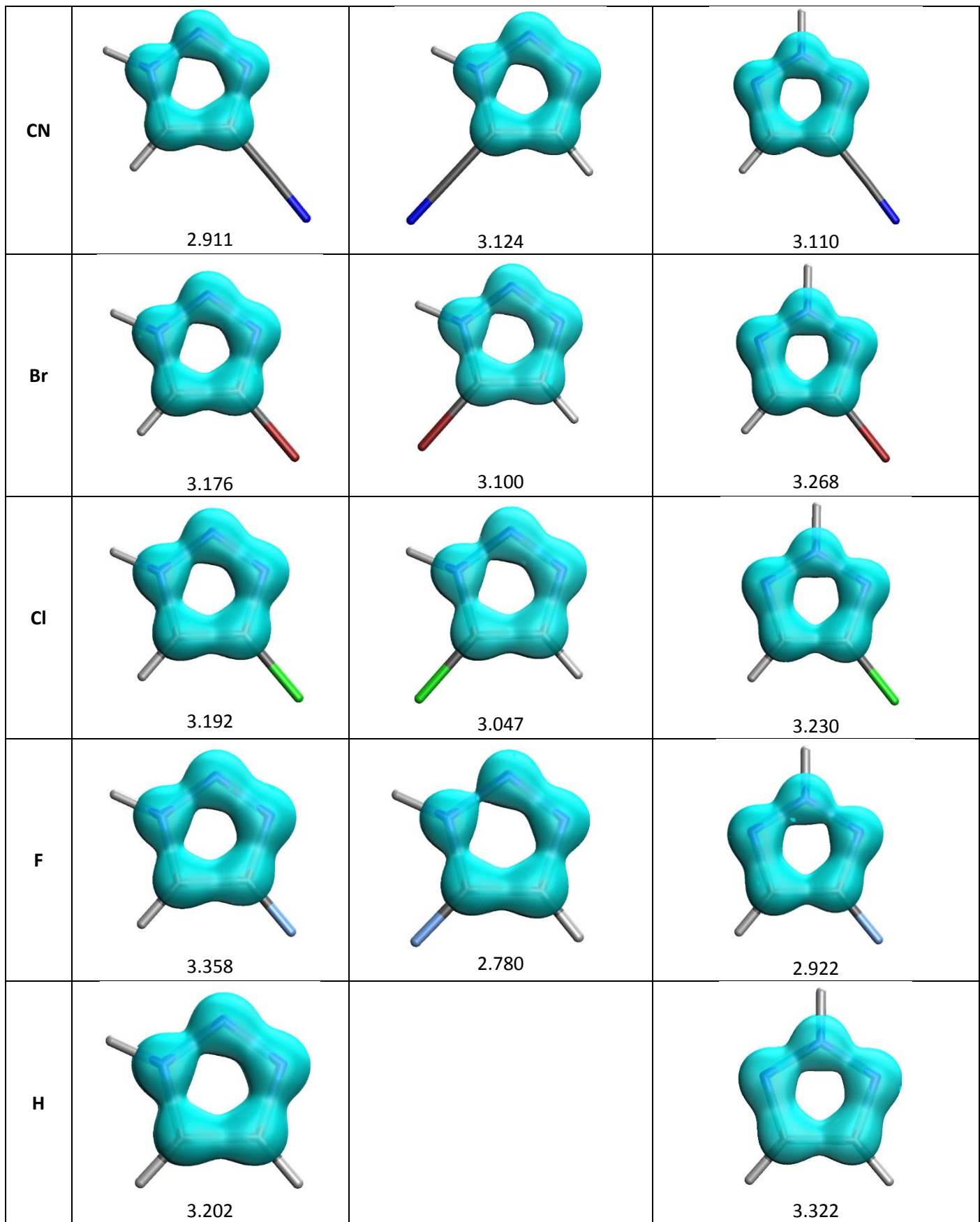


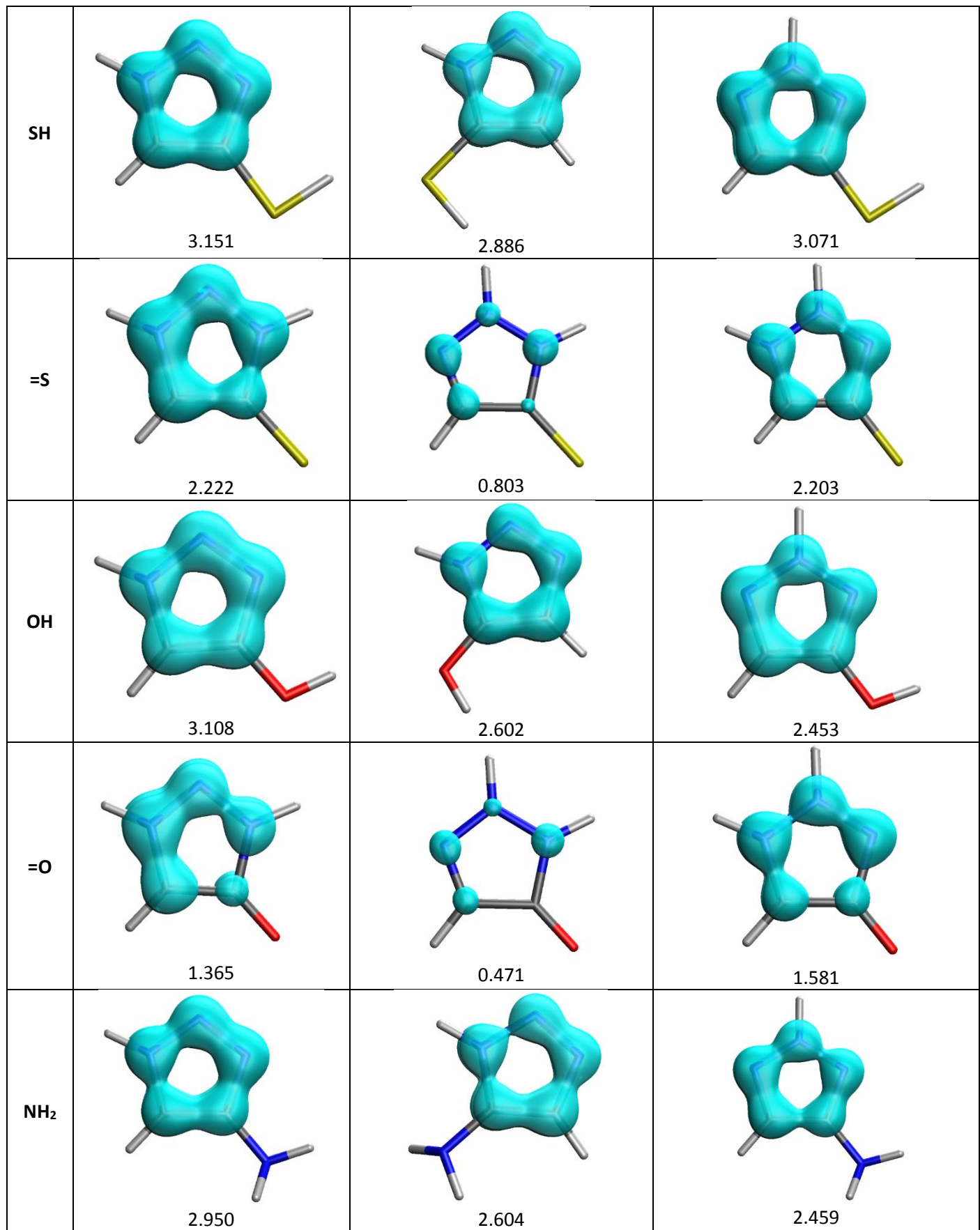


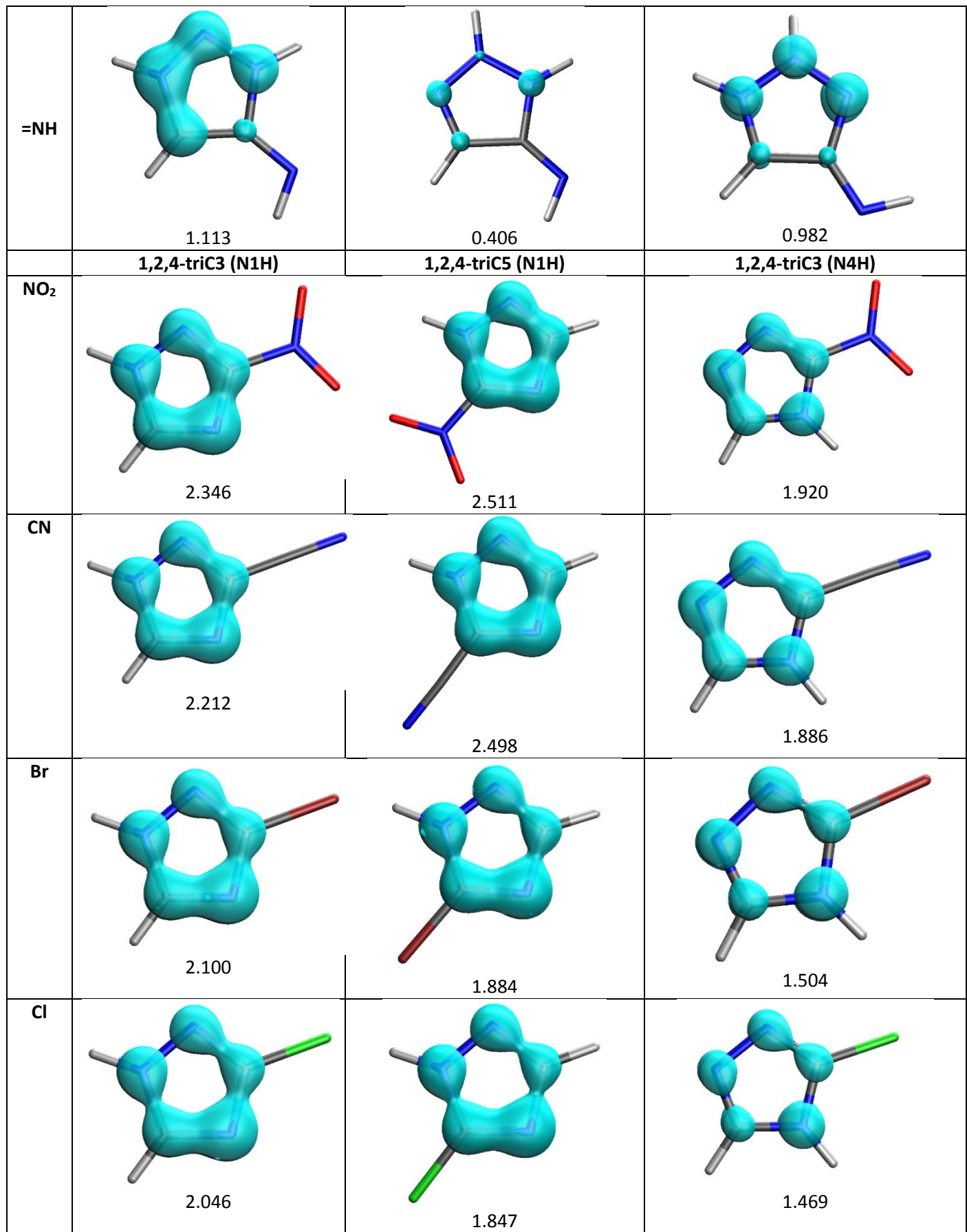


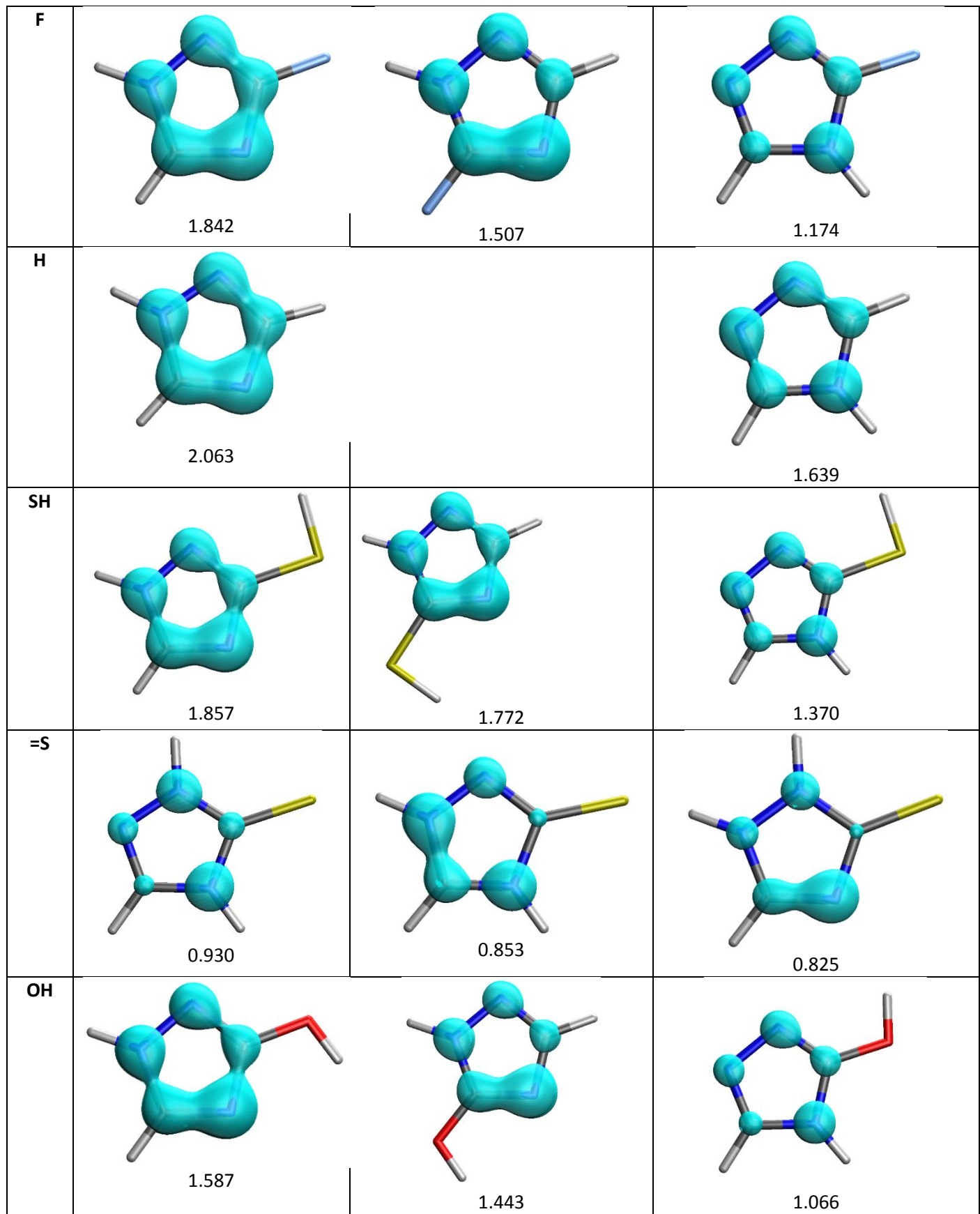


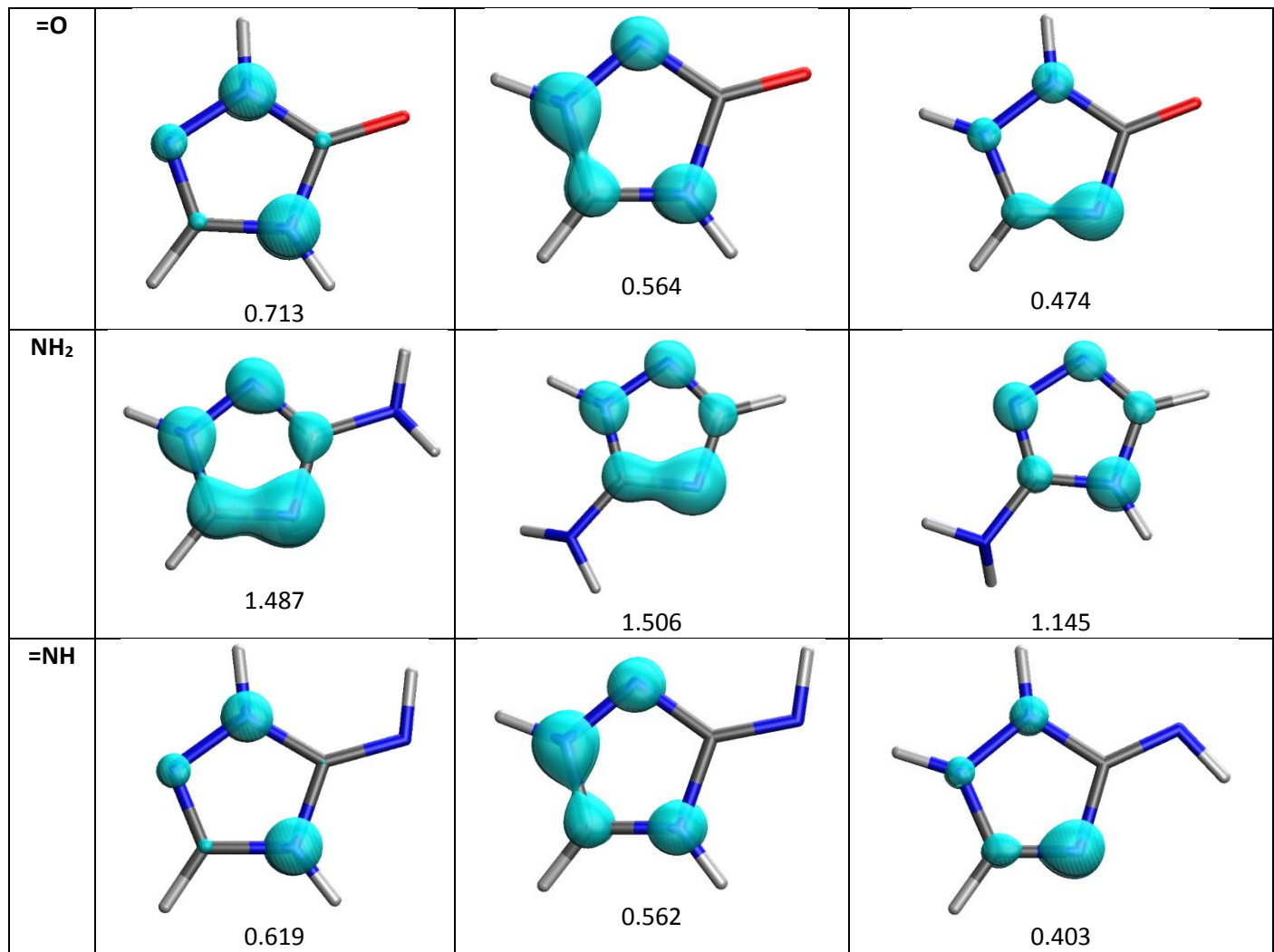
H	 2.529		
SH	 2.602	 2.322	
OH	 1.728	 2.160	
NH ₂	 2.459	 1.986	
	1,2,3-triC4 (N1H)	1,2,3-triC5 (N1H)	1,2,3-triC4 (N2H)
NO ₂	 2.992	 3.190	 3.028











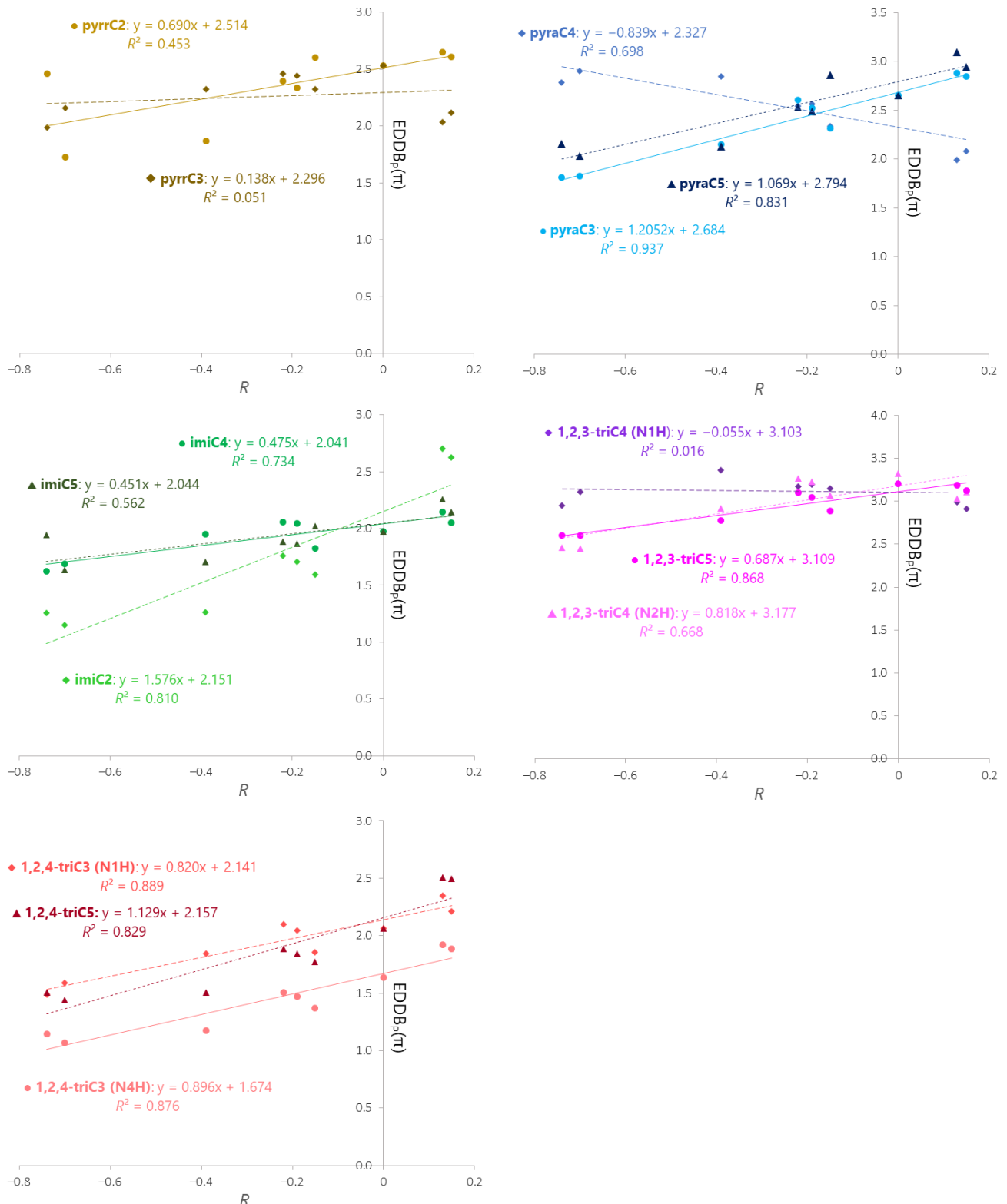
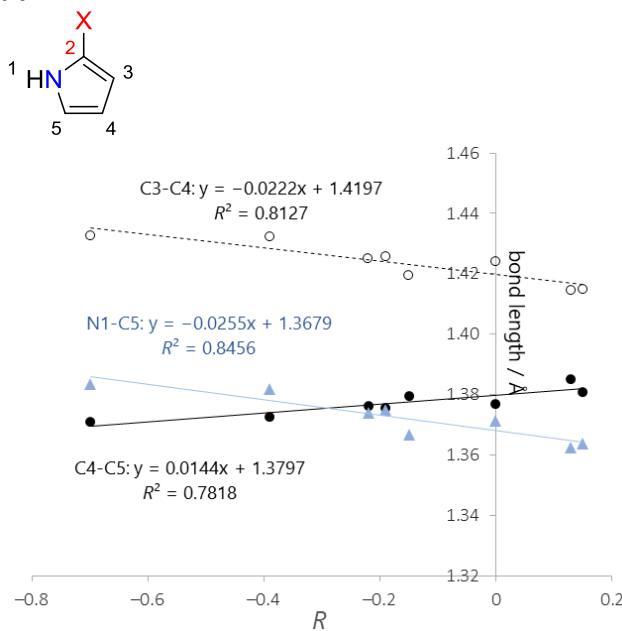
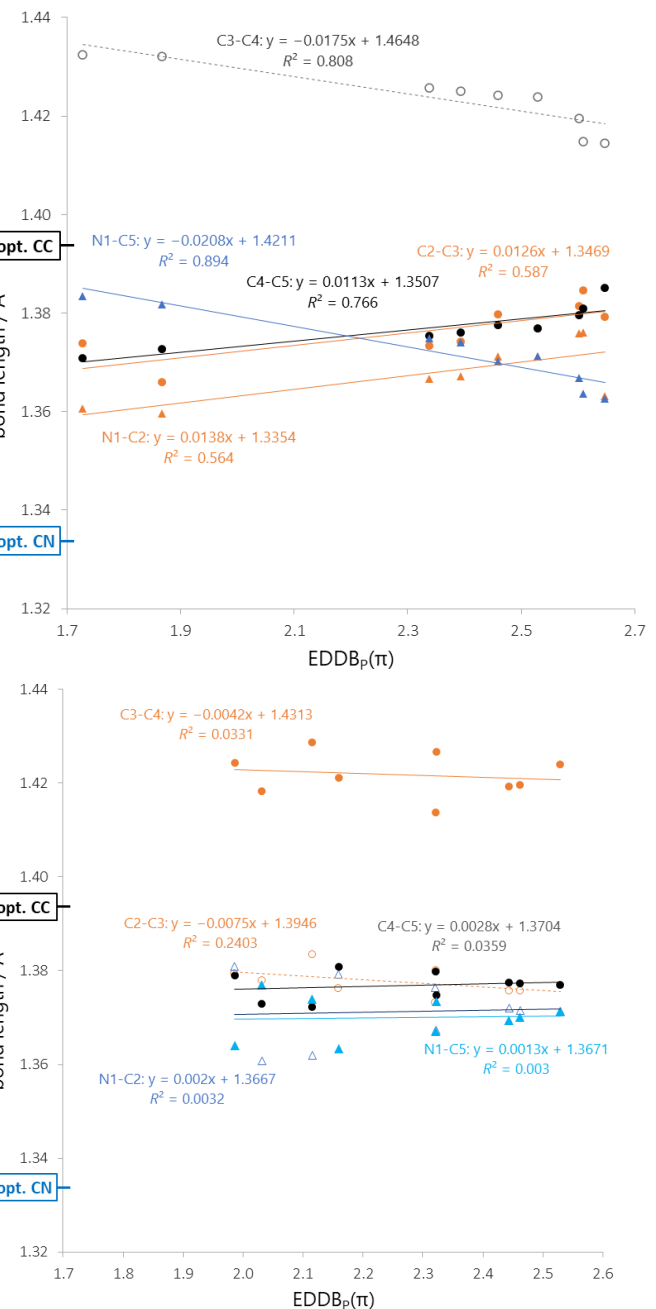
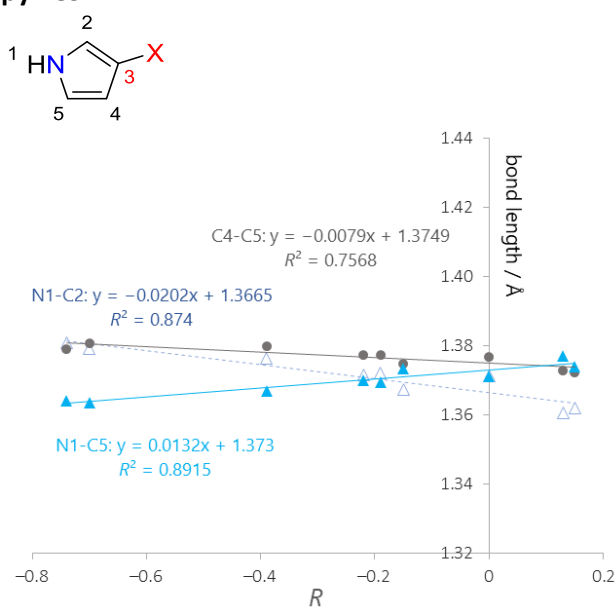


Figure S2. Relationships between $\text{EDDB}_P(\pi)$ and resonance substituent constant R .

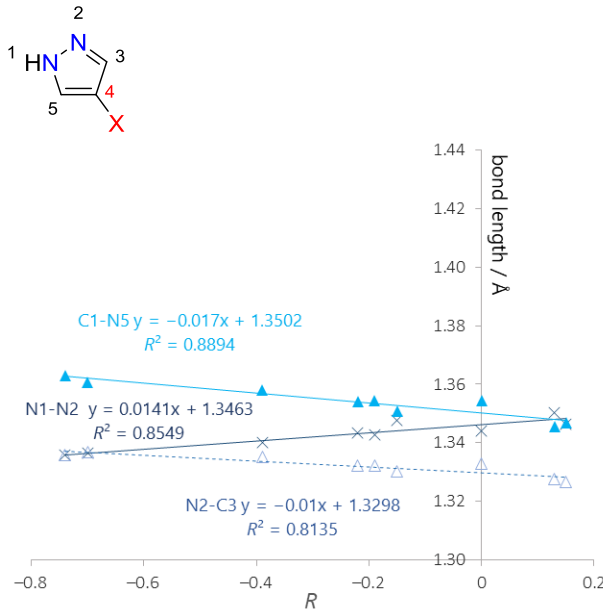
pyrrC2



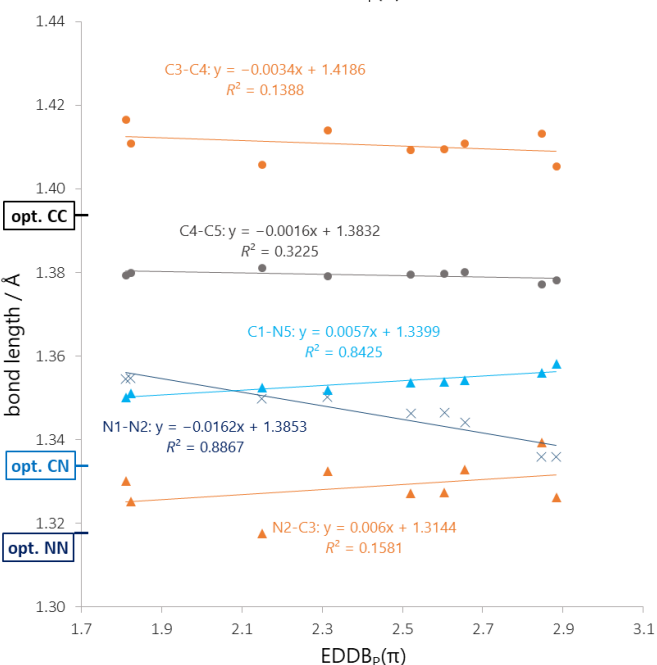
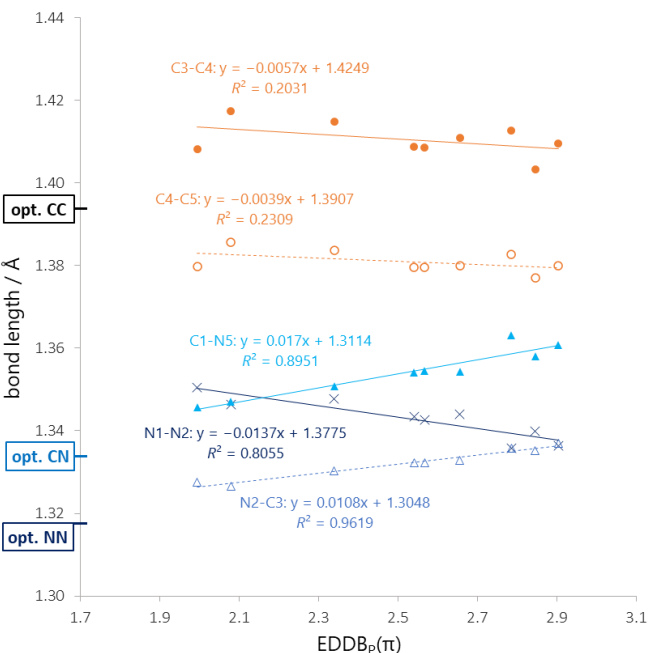
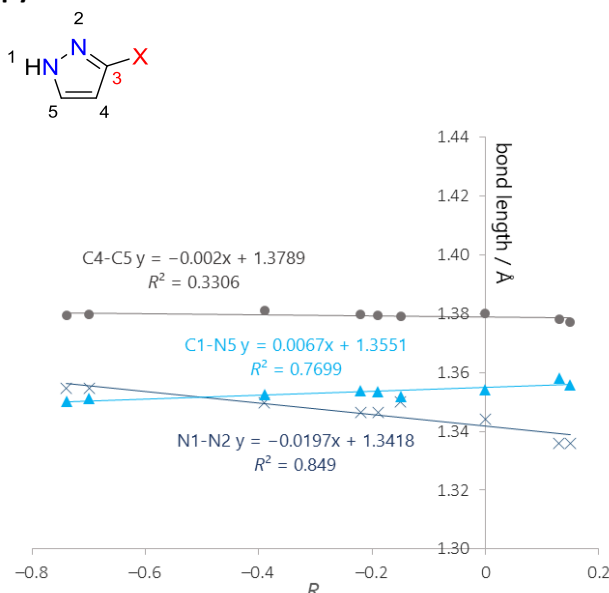
pyrrC3



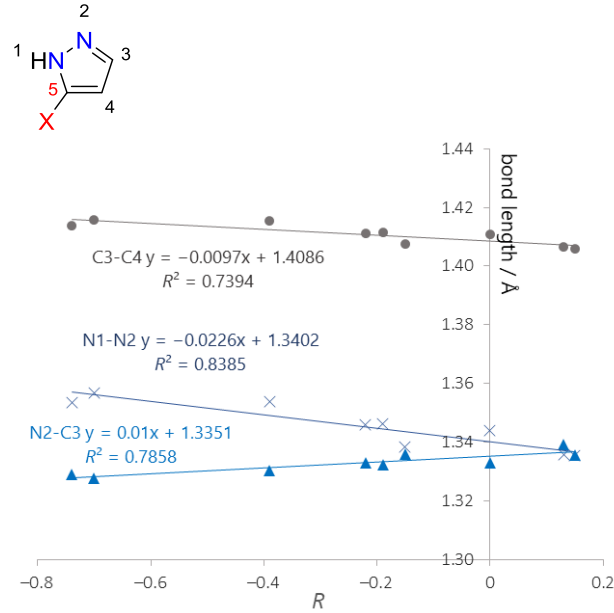
pyraC4



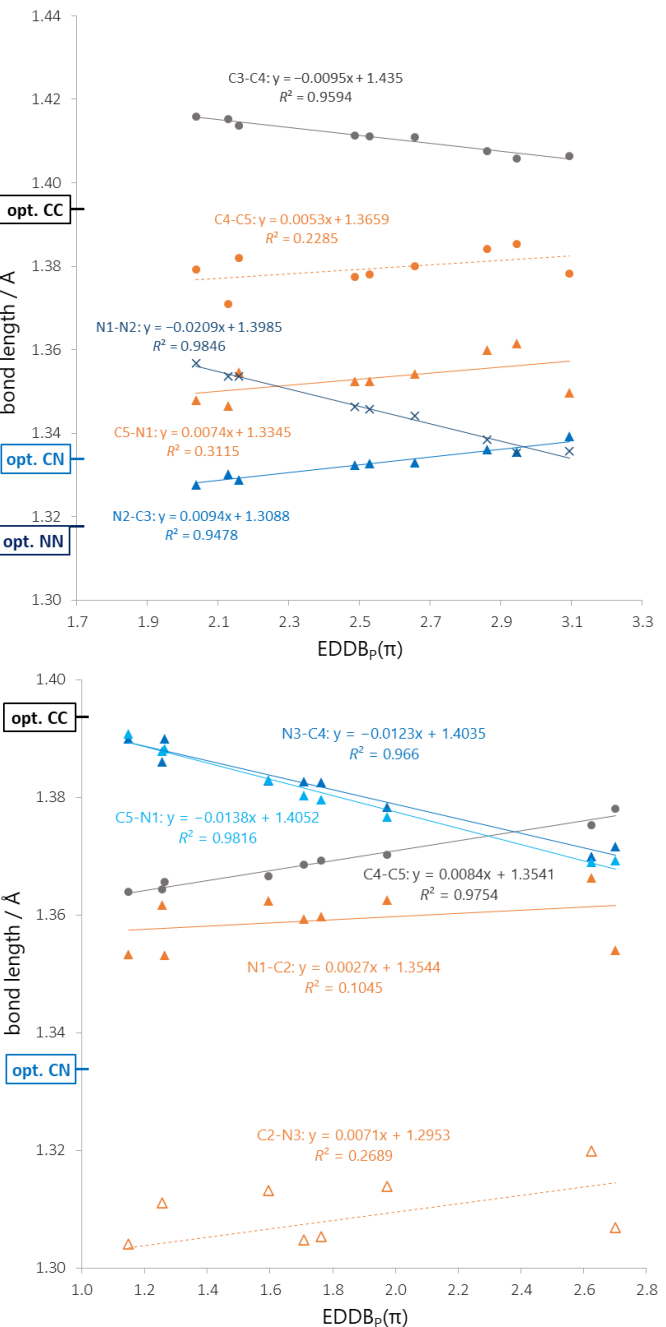
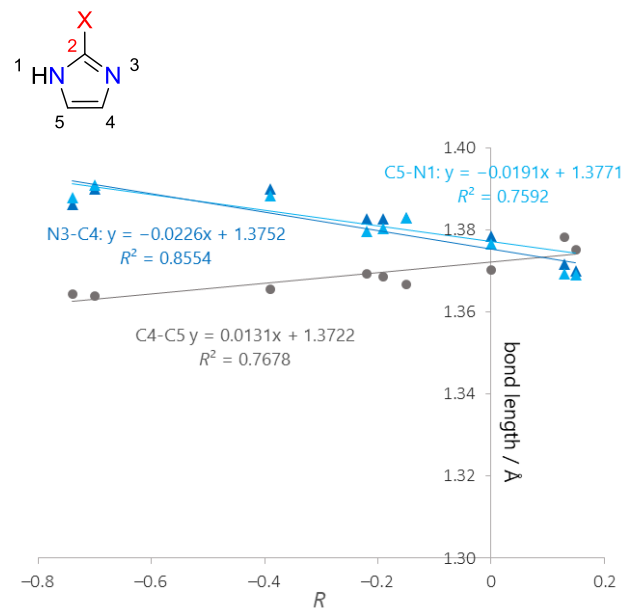
pyraC3



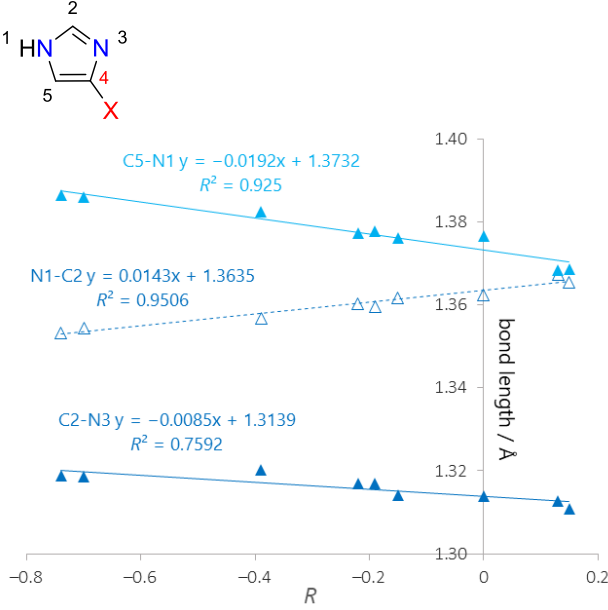
pyraC5



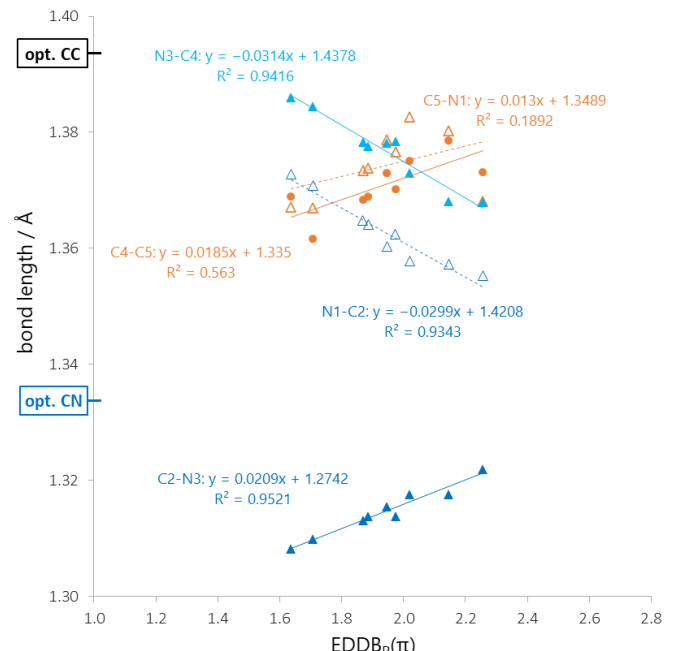
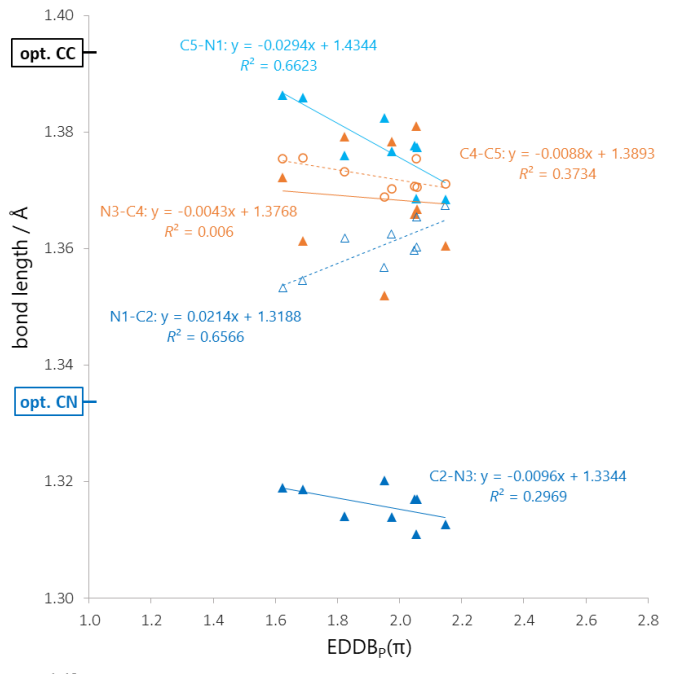
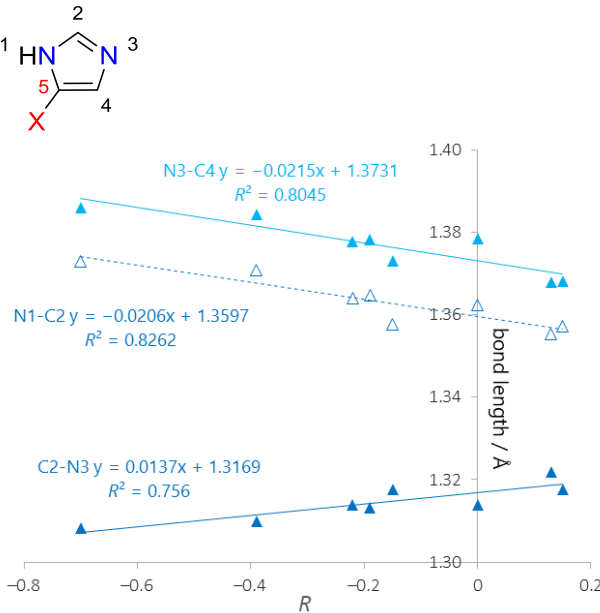
imiC2



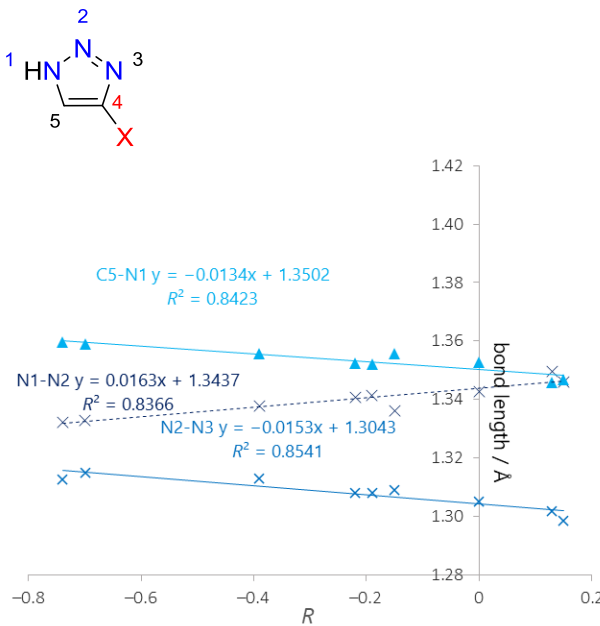
imic4



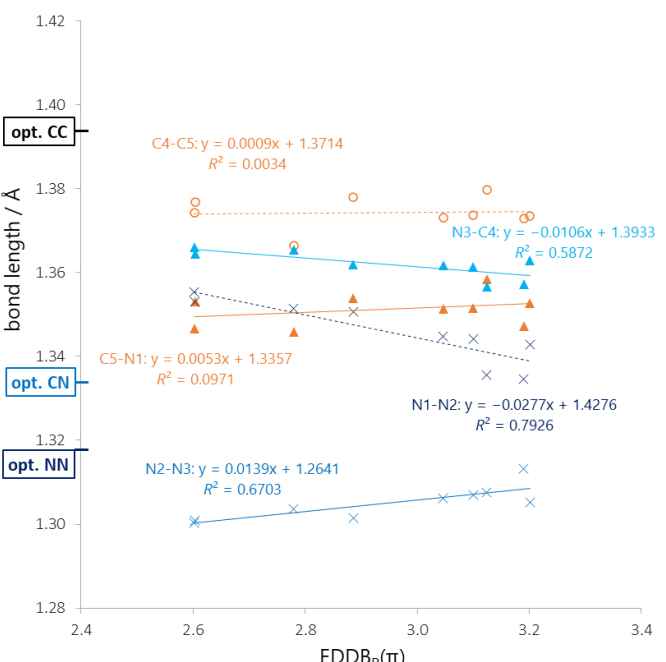
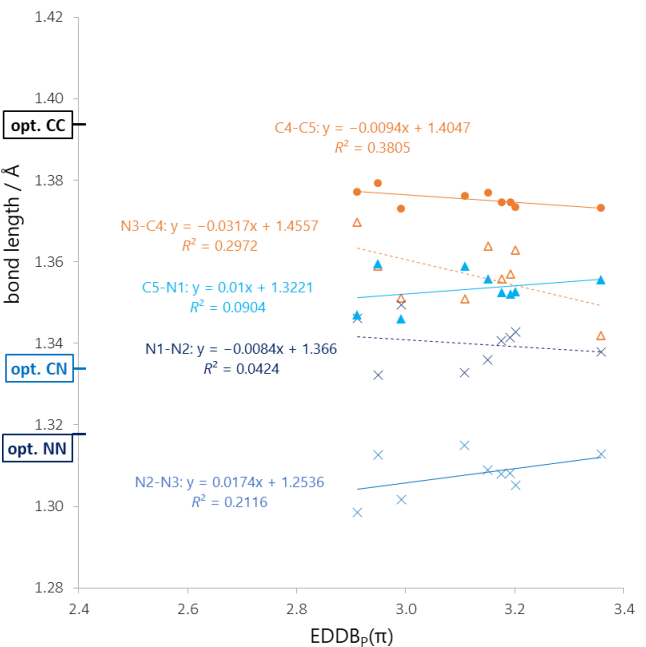
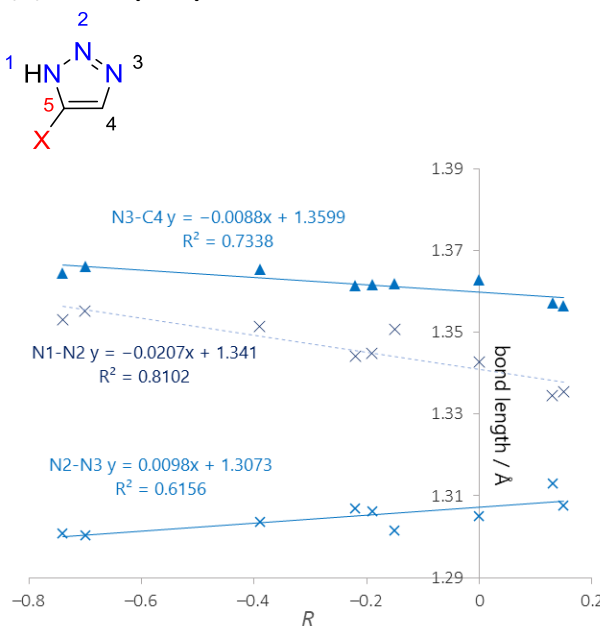
imic5



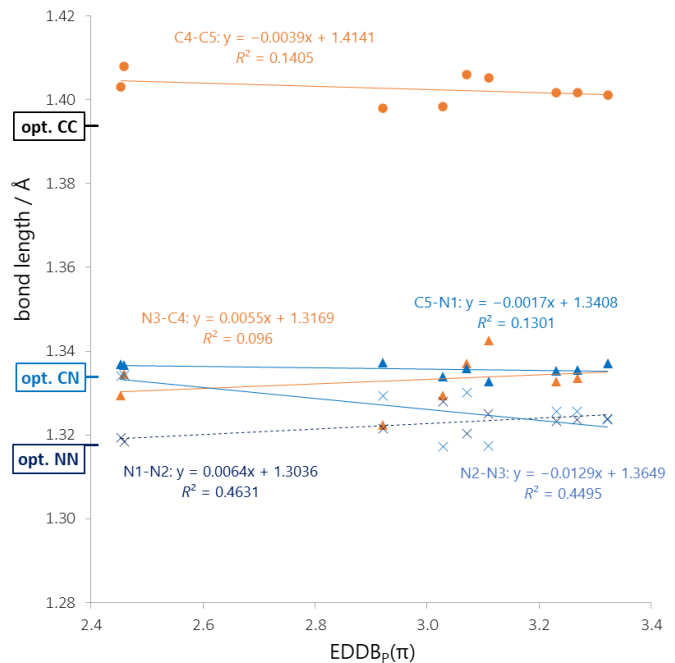
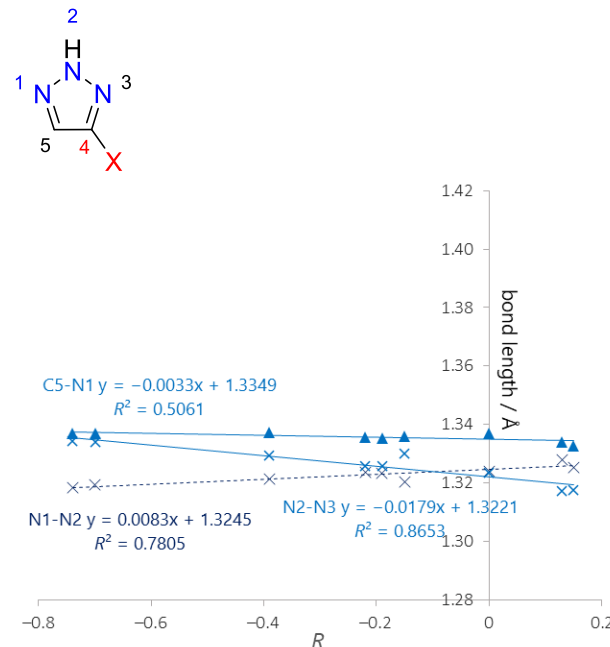
1,2,3-triC4 (N1H)



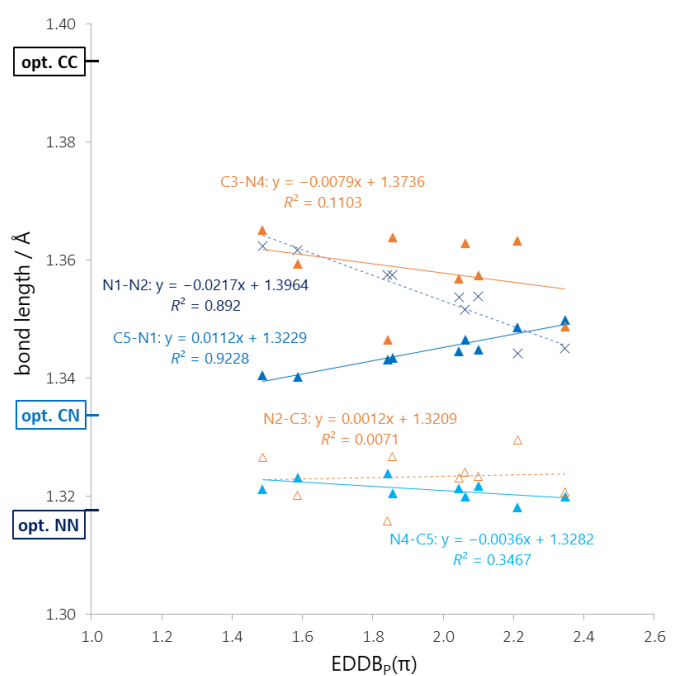
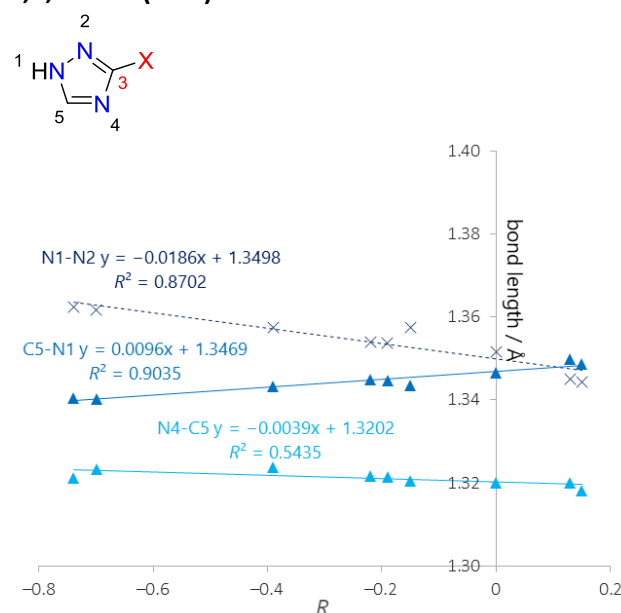
1,2,3-triC5 (N1H)



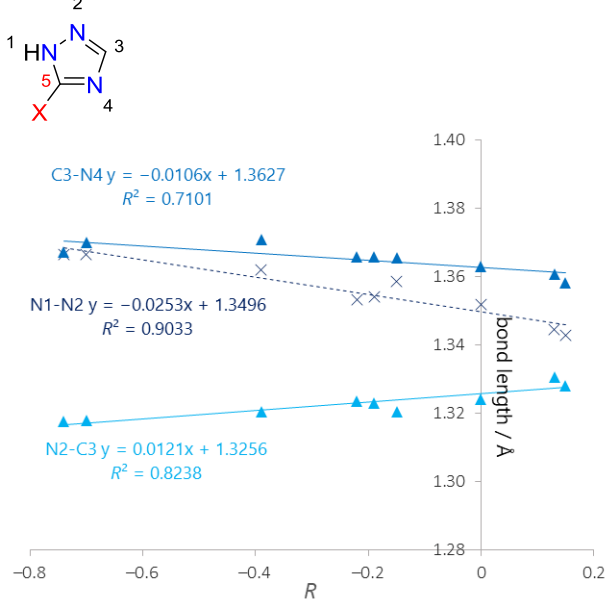
1,2,3-triC4 (N2H)



1,2,4-triC3 (N1H)



1,2,4-triC5



1,2,4-triC3 (N4H)

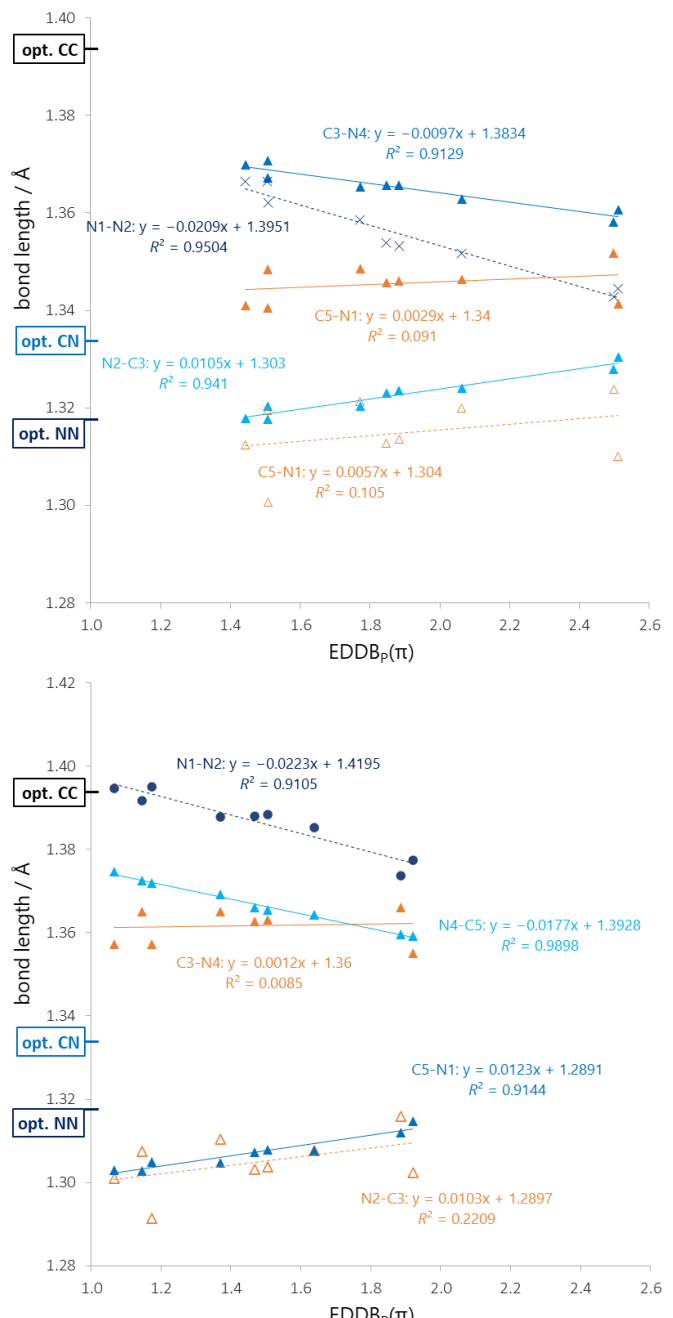
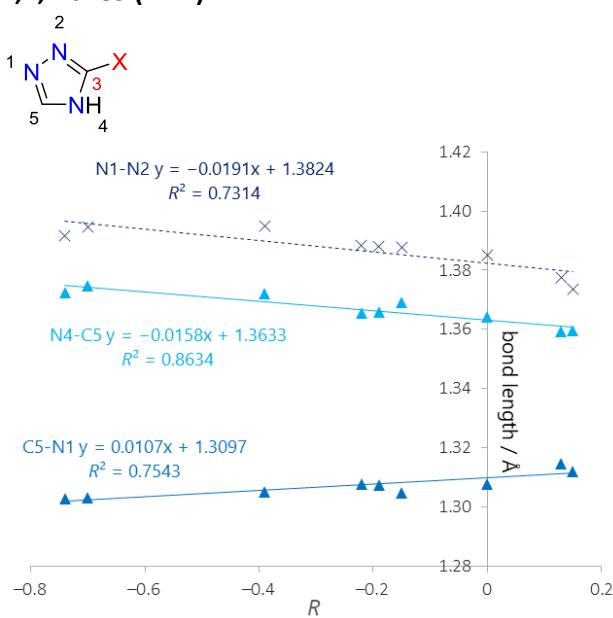


Figure S3. Relations between lengths of bonds In the ring and resonance R constants (left column) or the number of cyclically delocalized π -electrons, EDDB_P(π) (right column).

n in sp^n hybrids (NBO analysis)

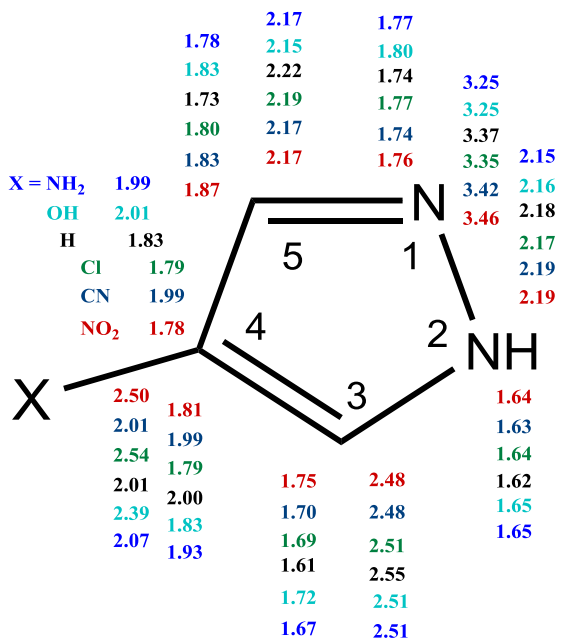


Figure S4. NBO analysis – natural hybrid orbital character of hybrids at ring atoms. Example – C4 substituted pyrazole derivatives (pyraC4).

Table S3. Crystallographic data found for monosubstituted compounds in CCSD.

	R	constant	N1-C2	C2-N3	N3-C4	C4-C5	C5-N1	ref
imic4	NO2	0.13	1.3673	1.3126	1.3605	1.3711	1.3685	KOMHAV [1]
	exp		1.3479	1.3187	1.3630	1.3614	1.3500	
	Br	-0.22	1.3602	1.3170	1.3668	1.3705	1.3773	LUDJAX [2]
	exp		1.3399	1.3242	1.3453	1.3606	1.3529	
imic2			N1-C2	C2-N3	N3-C4	C4-C5	C5-N1	
	NO2	0.15	1.3673	1.3126	1.3605	1.3711	1.3685	CELBAW [3]
	exp		1.3426	1.3178	1.3703	1.3756	1.3689	
	Cl	-0.19	1.3593	1.3047	1.3827	1.3686	1.3803	EJEGOS [4]
	exp		1.3243	1.3169	1.3833	1.3658	1.3796	
	NH2	-0.74	1.3617	1.3110	1.3861	1.3644	1.3879	CIVRUV [5]
pyrac4	exp-nh-co-nh-ph		1.3448	1.3235	1.3910	1.3475	1.3836	
			N1-N2	N2-C3	C3-C4	C4-C5	C1-N5	
	NO2	0.13	1.3504	1.3275	1.4082	1.3797	1.3456	WIKZUL [6]
	exp		1.3588	1.3283	1.3905	1.3796	1.3259	
	NH2	-0.74	1.3357	1.3358	1.4127	1.3828	1.3631	HIWJIG [7]
1,2,3-triC4 (N1H)	exp		1.3457	1.3299	1.3879	1.3859	1.3540	
			N1-N2	N2-N3	N3-C4	C4-C5	C5-N1	
	NO2	0.13						RAMVUW [8]
	exp		1.3451	1.3025	1.3410	1.3631	1.3226	
1,2,4-triC3 (N1H)	SF5	0.12	1.3427	1.3136	1.3550	1.3683	1.3324	LIPTOU [9]
	NO2	0.13	1.3450	1.3207	1.3487	1.3199	1.3499	CIFROY [10]
	exp 1		1.3502	1.3131	1.3428	1.3290	1.3325	
	Br	-0.22	1.3539	1.3234	1.3574	1.3217	1.3449	BIJLEL01 [11]
	exp		1.3549	1.3073	1.3458	1.3232	1.3193	
	Cl	-0.19	1.3537	1.3231	1.3569	1.3214	1.3446	CLTRZL [12]
1,2,4-triC3 (N4H)	exp		1.3671	1.3133	1.3500	1.3291	1.3157	
			N1-N2	N2-C3	C3-N4	N4-C5	C5-N1	
	NH2	-0.74	1.3917	1.3074	1.3650	1.3724	1.3028	CEBPEH [13]
	exp		1.3875	1.3375	1.3465	1.3643	1.2943	

- [1] [10.1107/S0108270191008065](https://doi.org/10.1107/S0108270191008065), [2] [10.5517/cc1j0ndl](https://doi.org/10.5517/cc1j0ndl), [3] [10.1107/S010827018400384X](https://doi.org/10.1107/S010827018400384X), [4] [10.5517/ccdc.csd.cc25wqd6](https://doi.org/10.5517/ccdc.csd.cc25wqd6),
 [5] [10.5517/ccq5bfm](https://doi.org/10.5517/ccq5bfm), [6] [10.1107/S0108768194004180](https://doi.org/10.1107/S0108768194004180), [7] [10.5517/cc3tyys](https://doi.org/10.5517/cc3tyys), [8] [10.5517/cc52rnrm](https://doi.org/10.5517/cc52rnrm), [9] [10.1021/ol701602a](https://doi.org/10.1021/ol701602a),
 [10] G.Evrard, F.Durant, A.Michel, J.G.Fripiat, J.L.Closset, A.Copin, *Bull. Soc. Chim. Belg.* **1984**, 93, 233, [11]
[10.5517/cc5dn4b](https://doi.org/10.5517/cc5dn4b), [12] M.S.Idrissi, M.Senechal, H.Sauvaitre, M.Cotrait, C.Garrigou-Lagrange, *J.Chim.Phys.*, **1980**, 77, 195,
 [13] [10.5517/ccdc.csd.cczcy5f](https://doi.org/10.5517/ccdc.csd.cczcy5f)

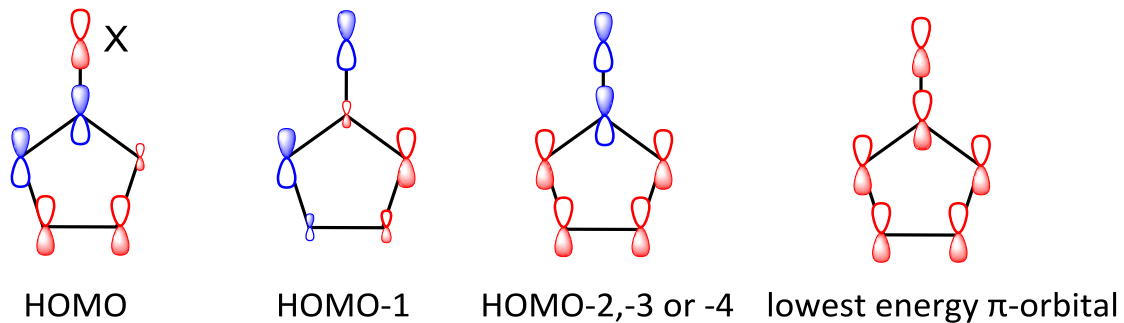
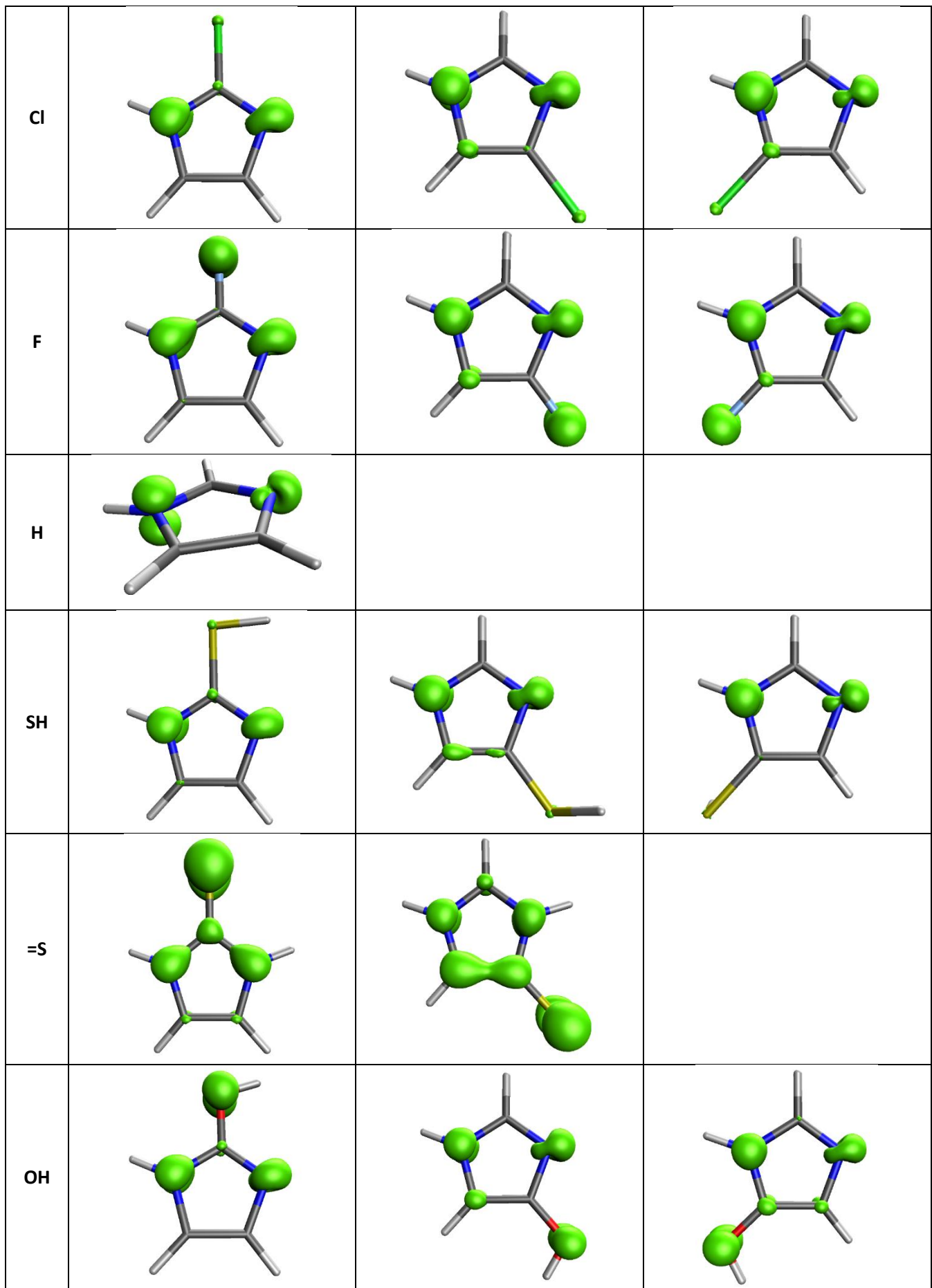
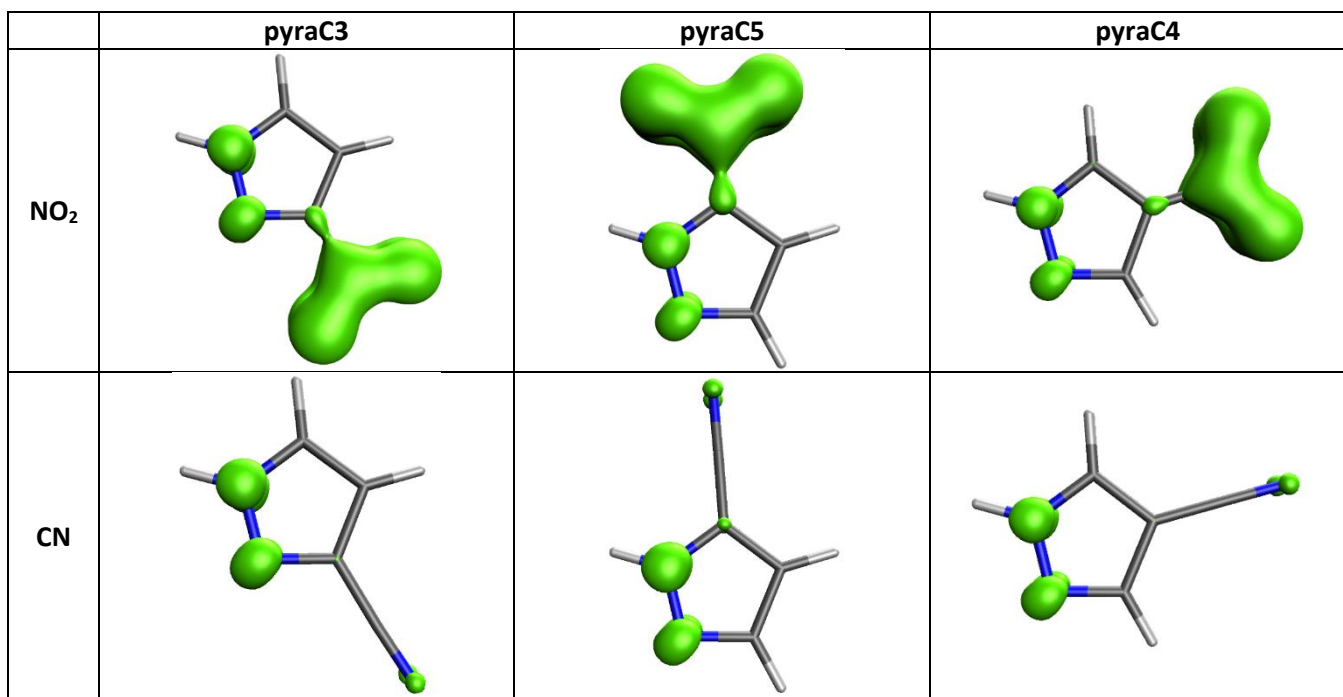
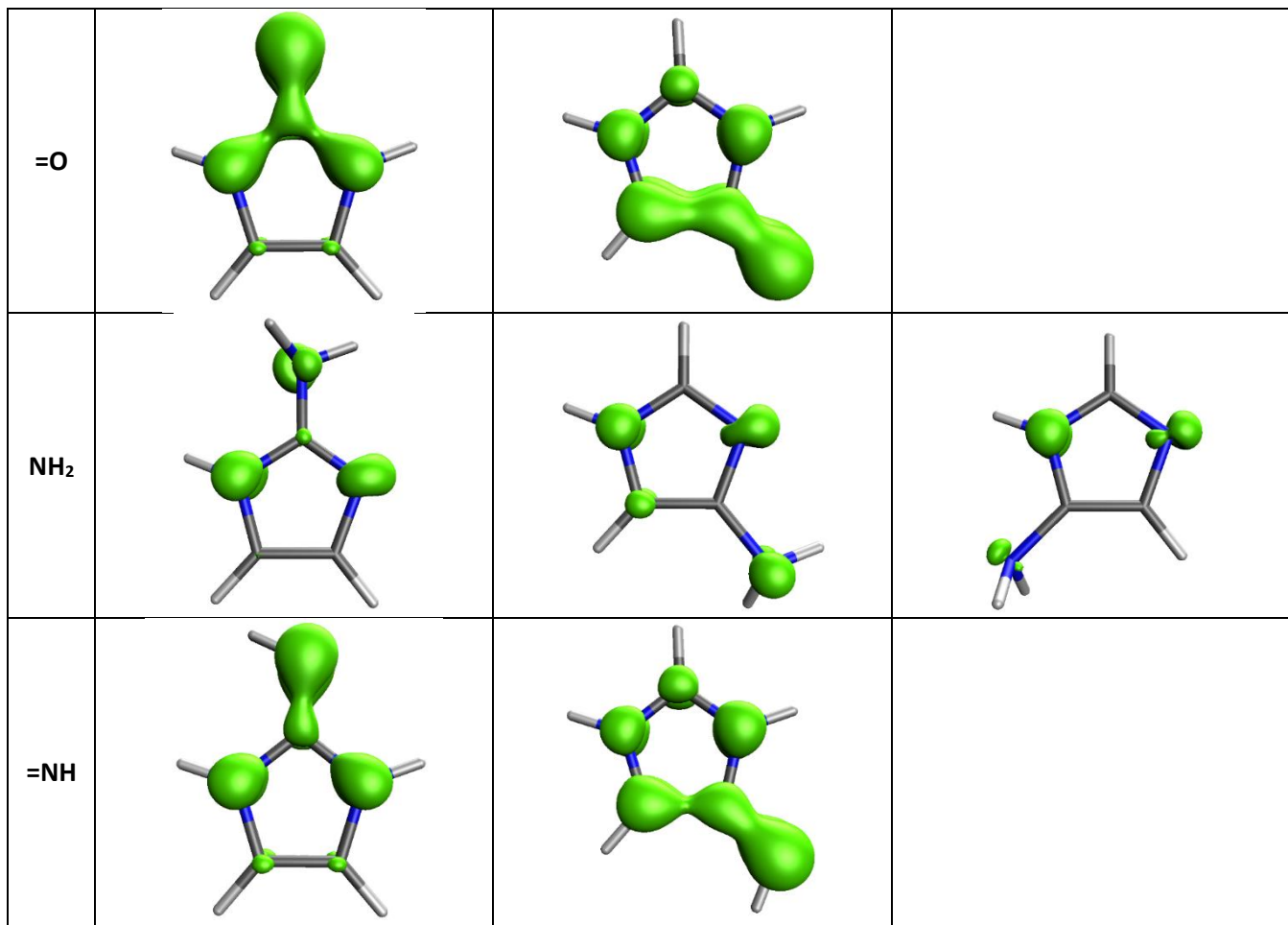


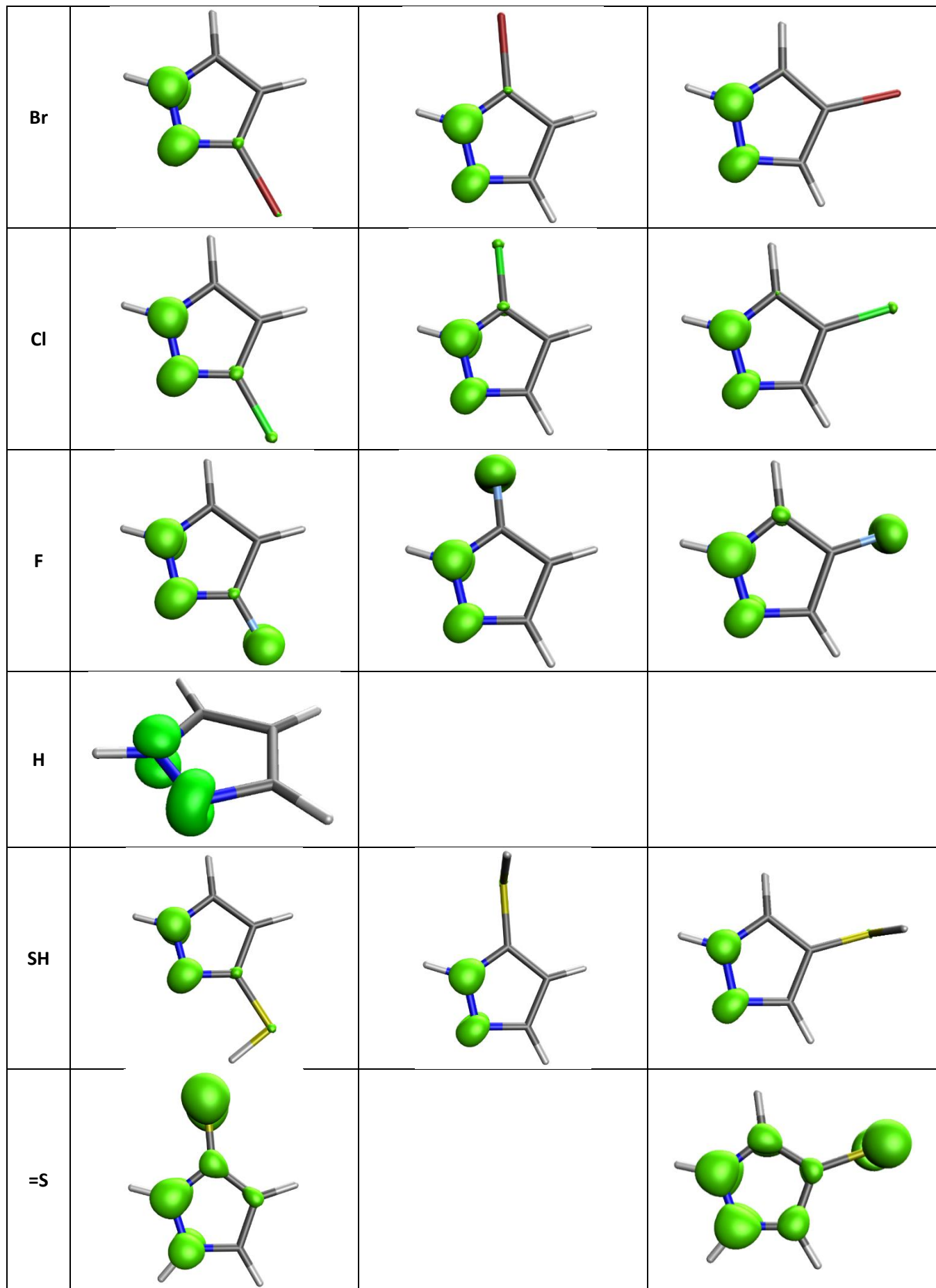
Figure S5. π -Orbital shapes independent of X substituent type.

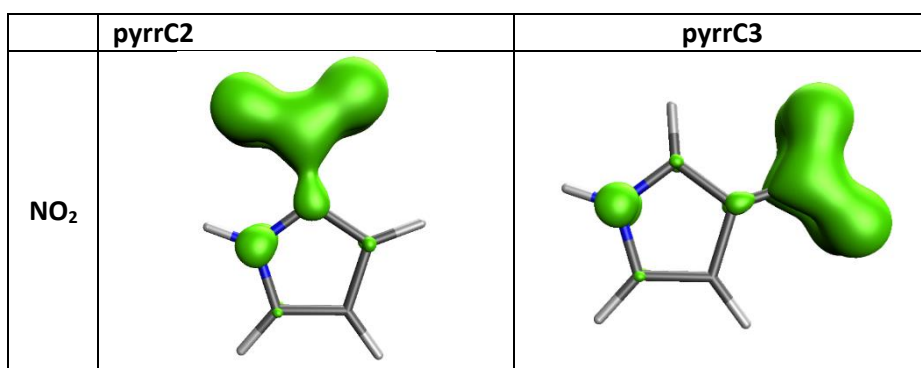
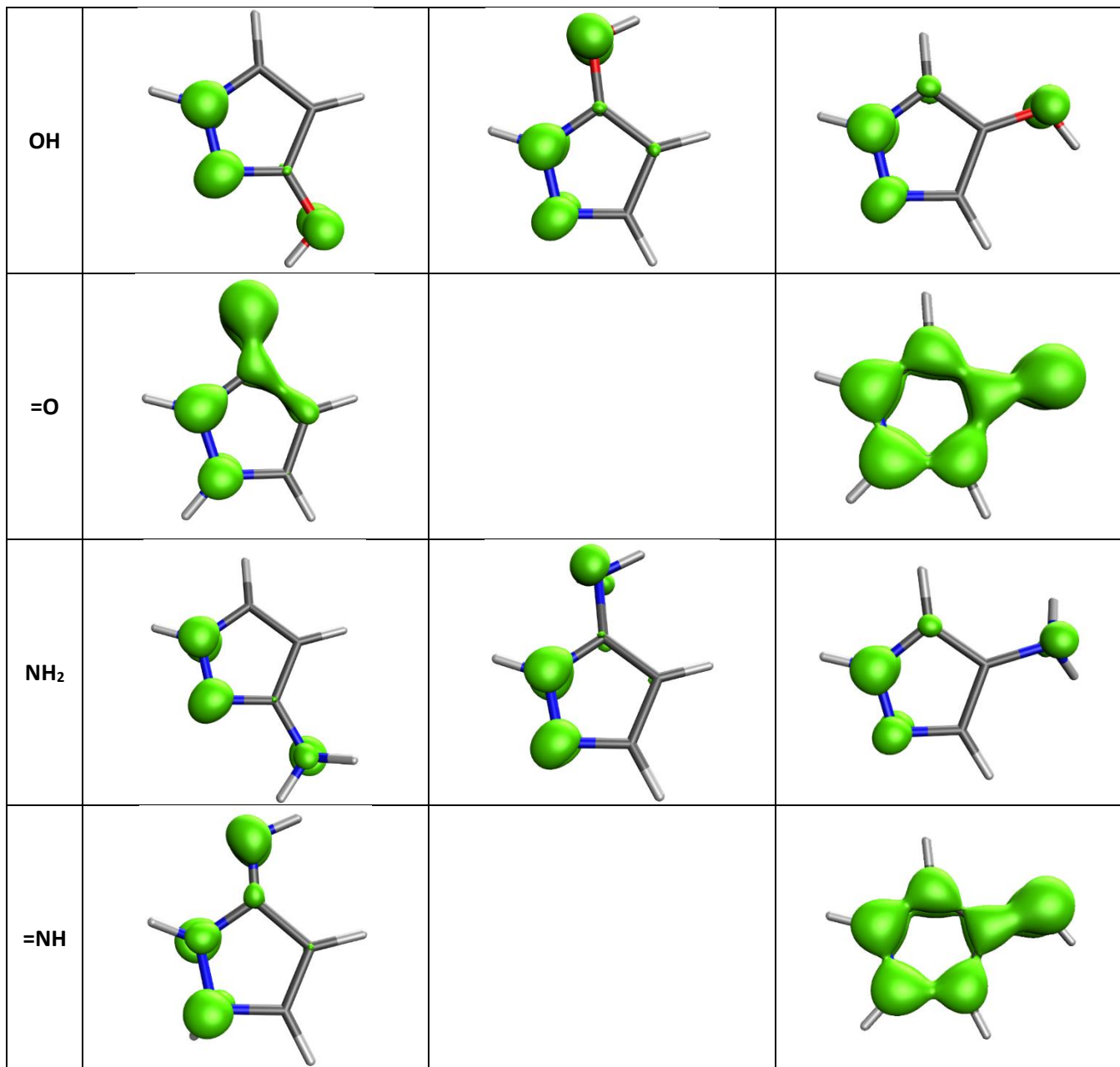
Table S4. Isosurfaces of EDDB_{G-P} function (0.02 electrons) – a visual representation of non-cyclic electron delocalization.

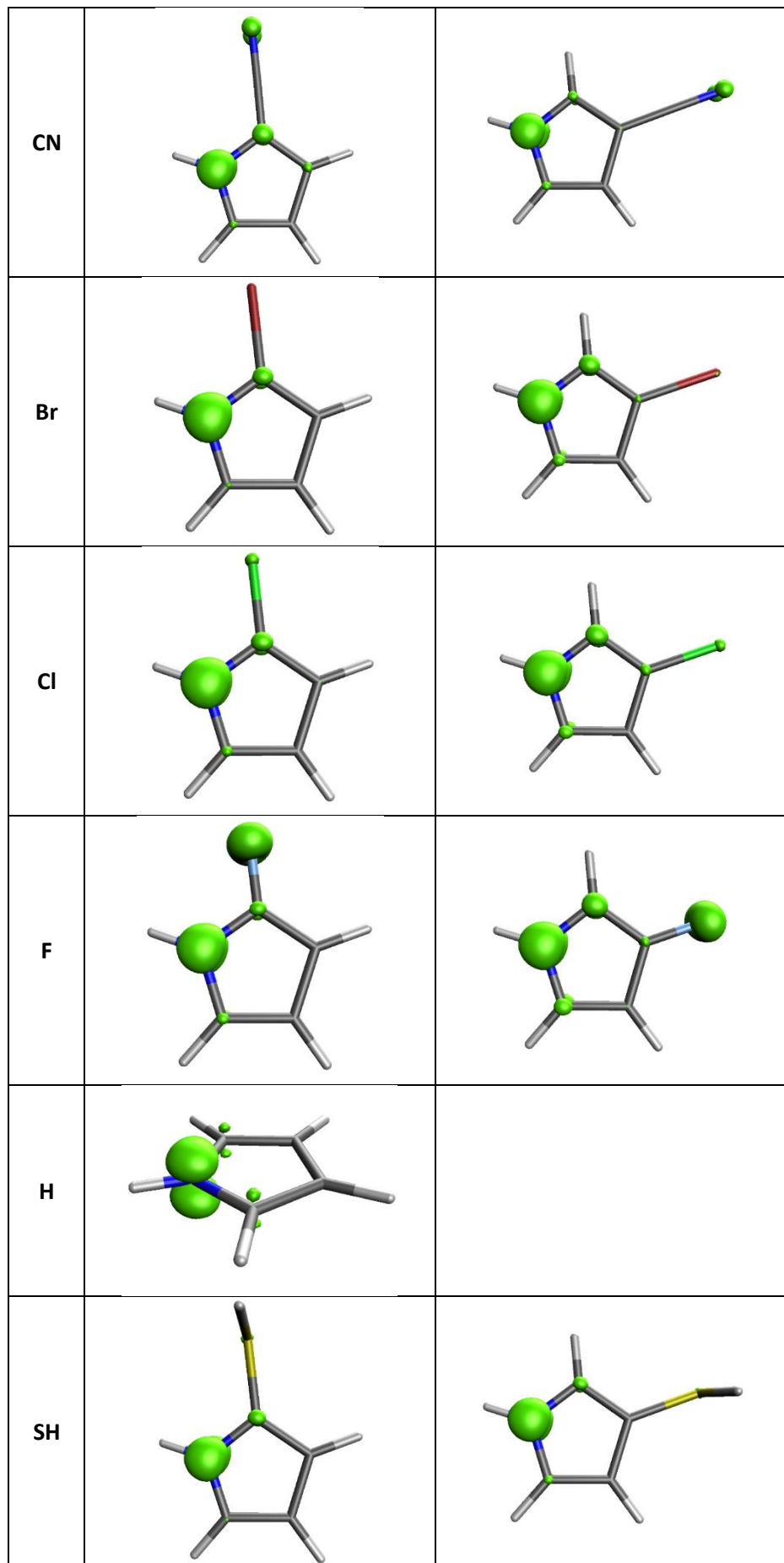
X	imiC2	imiC4	imiC5
NO ₂			
CN			
Br			

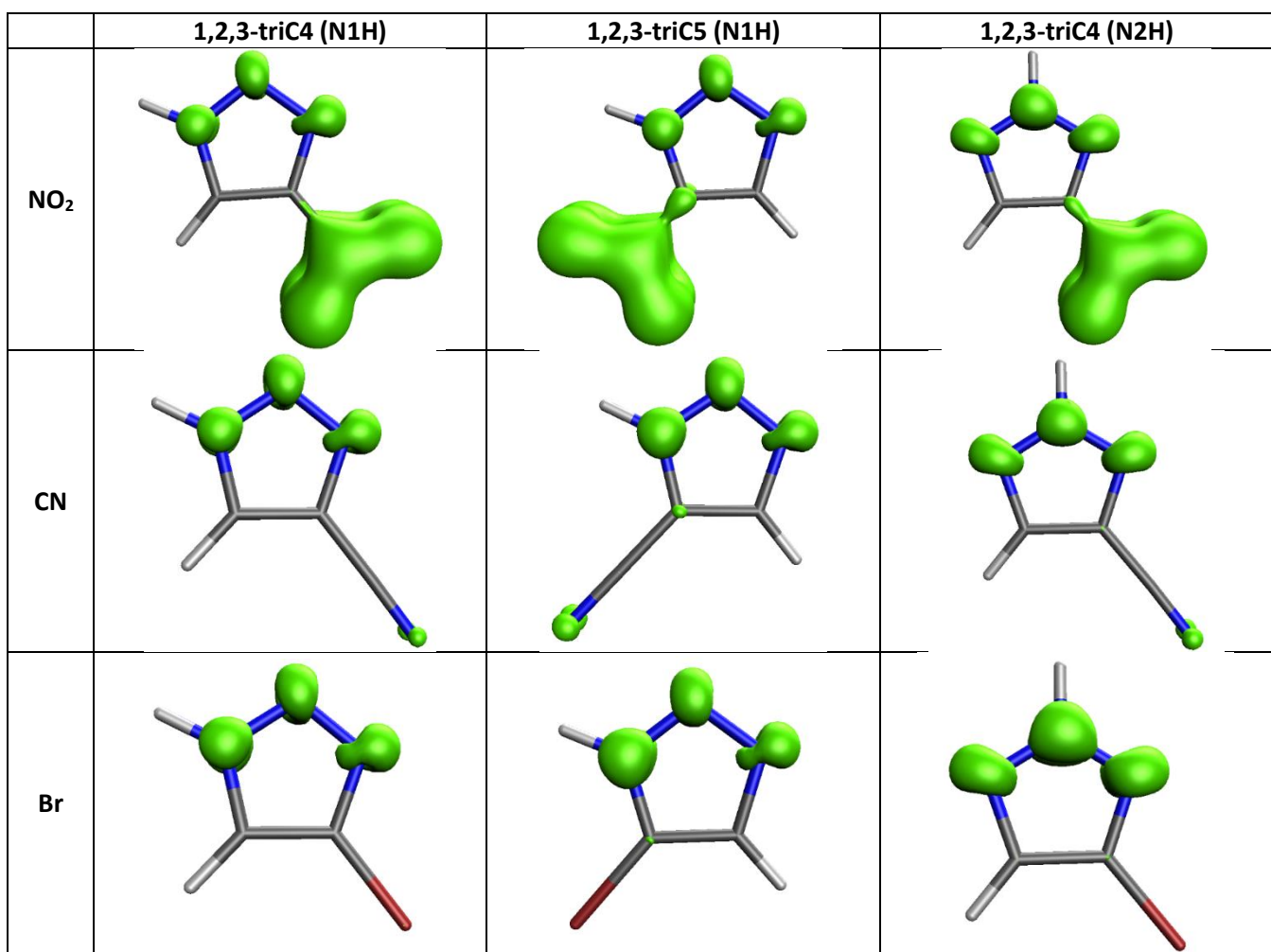
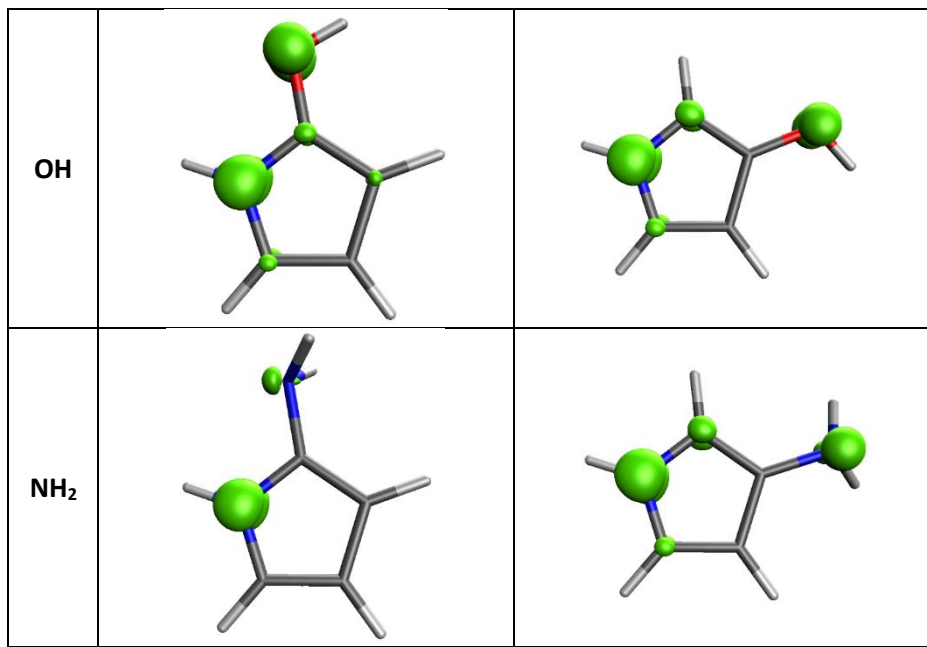


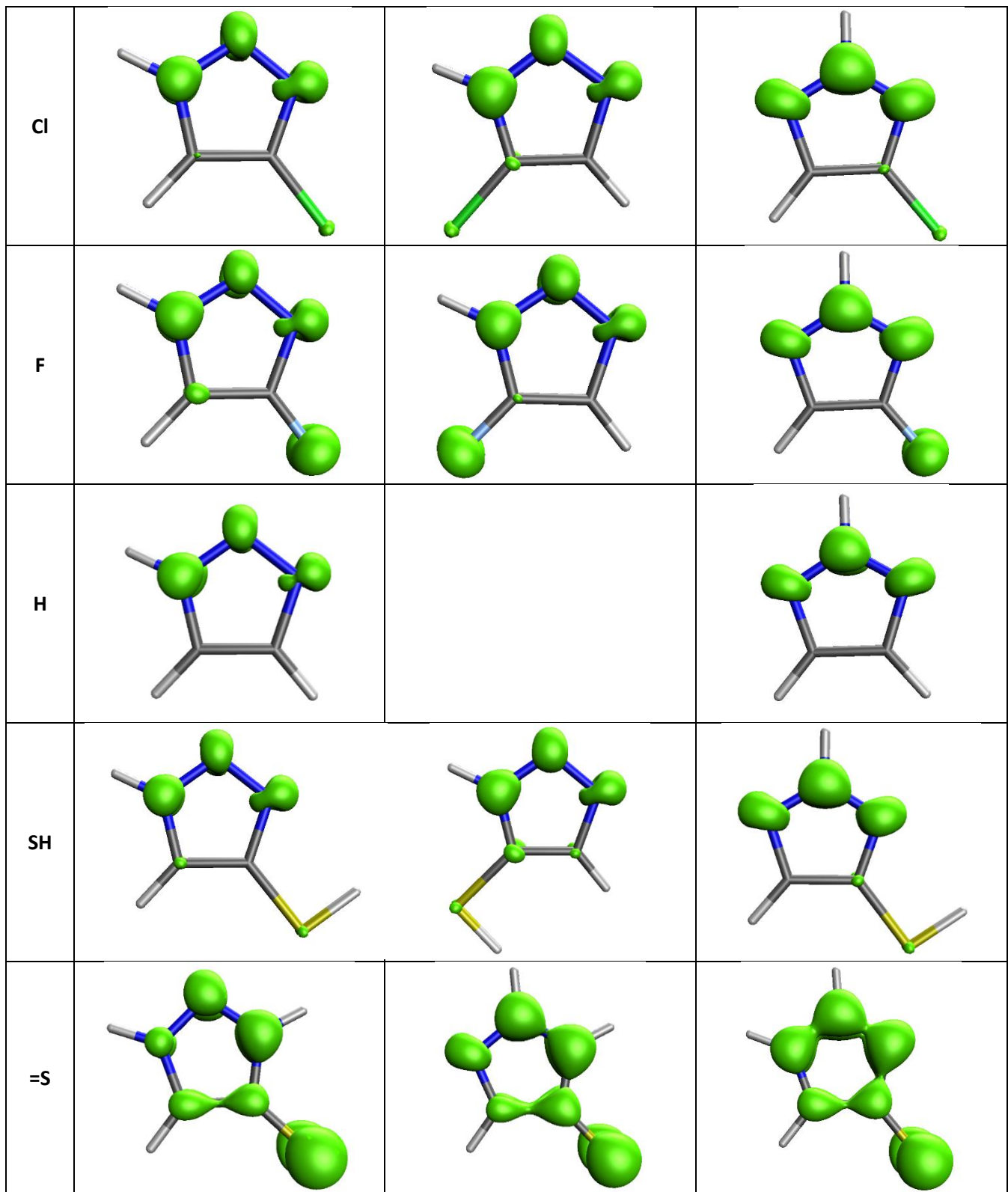


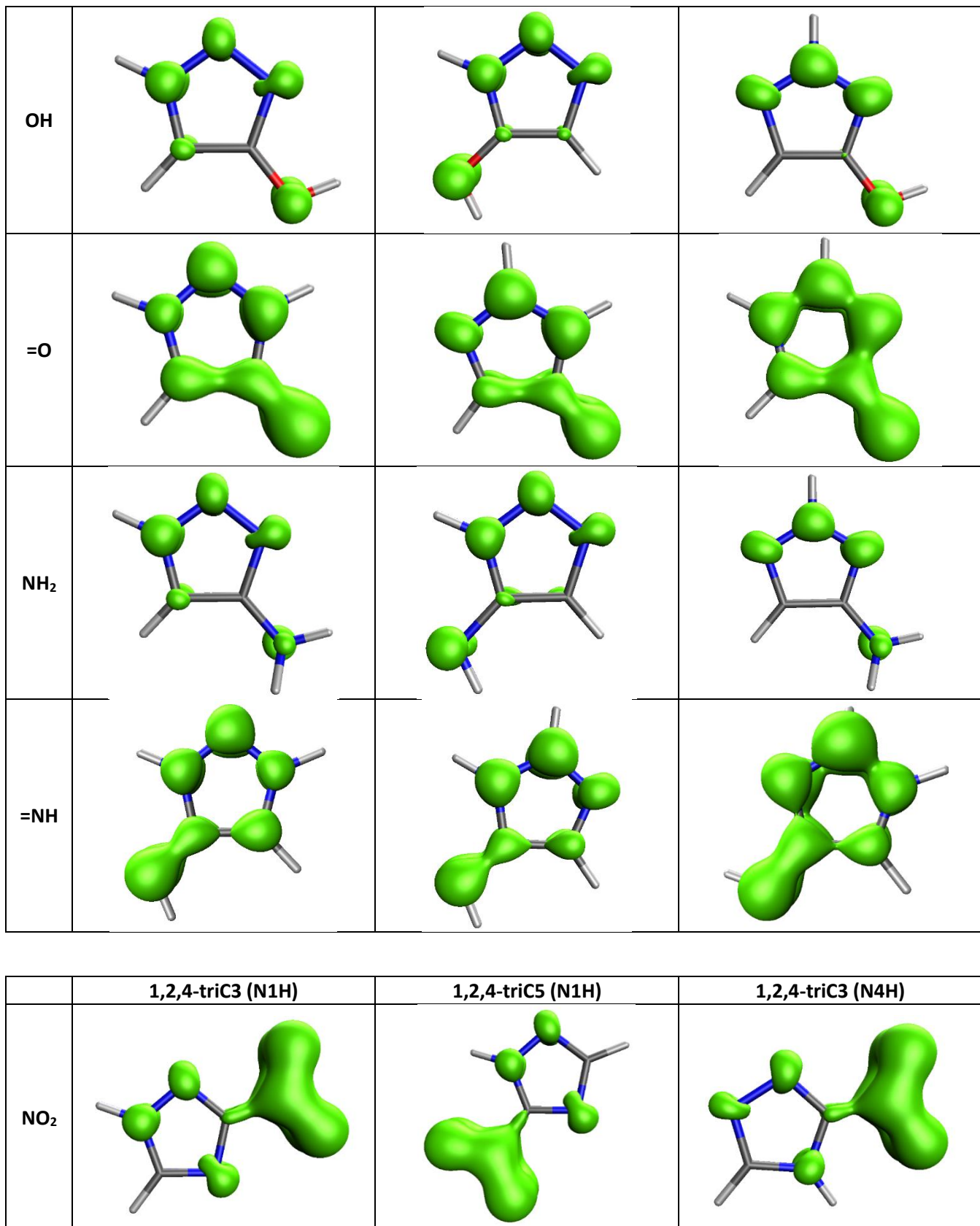


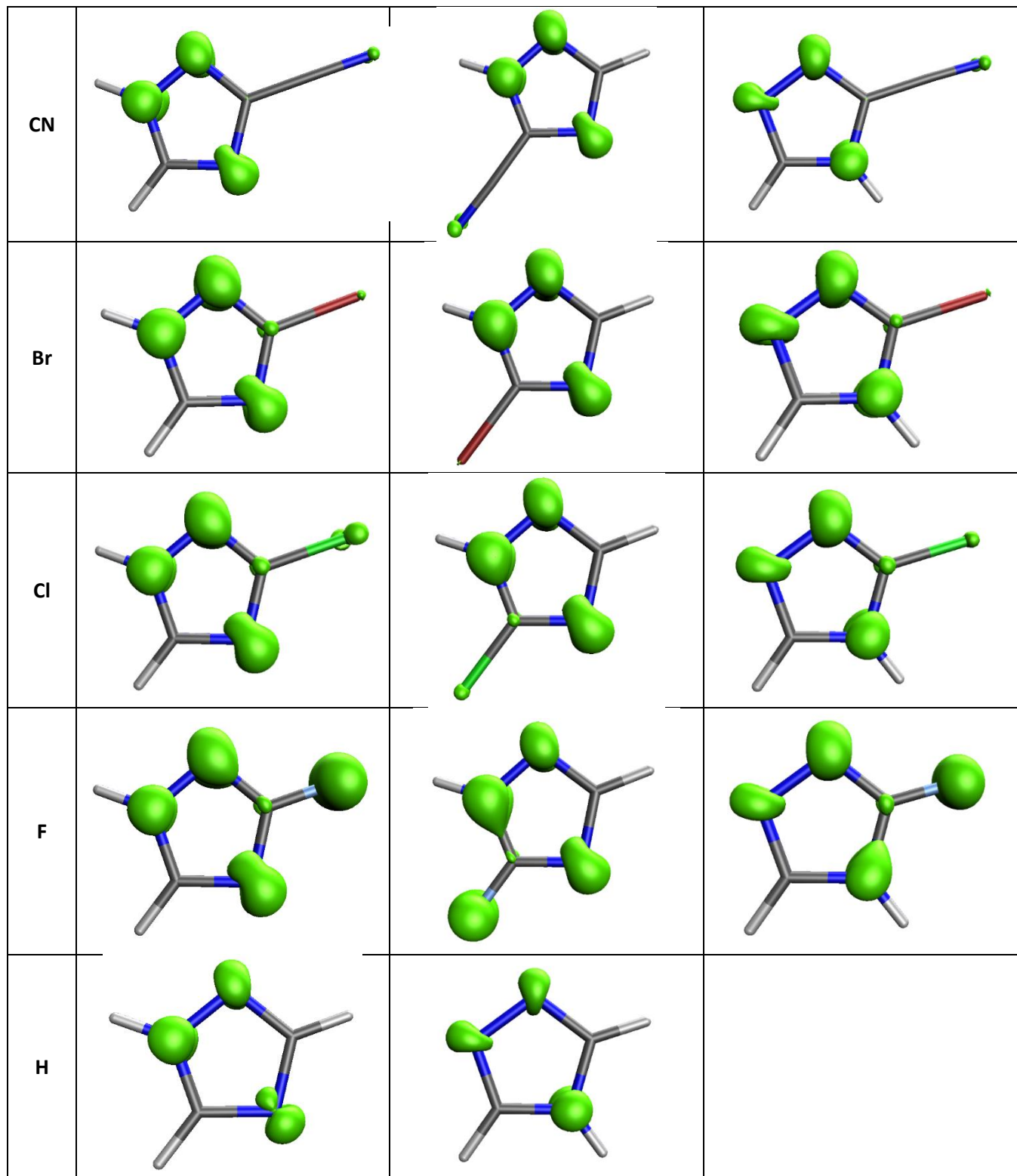


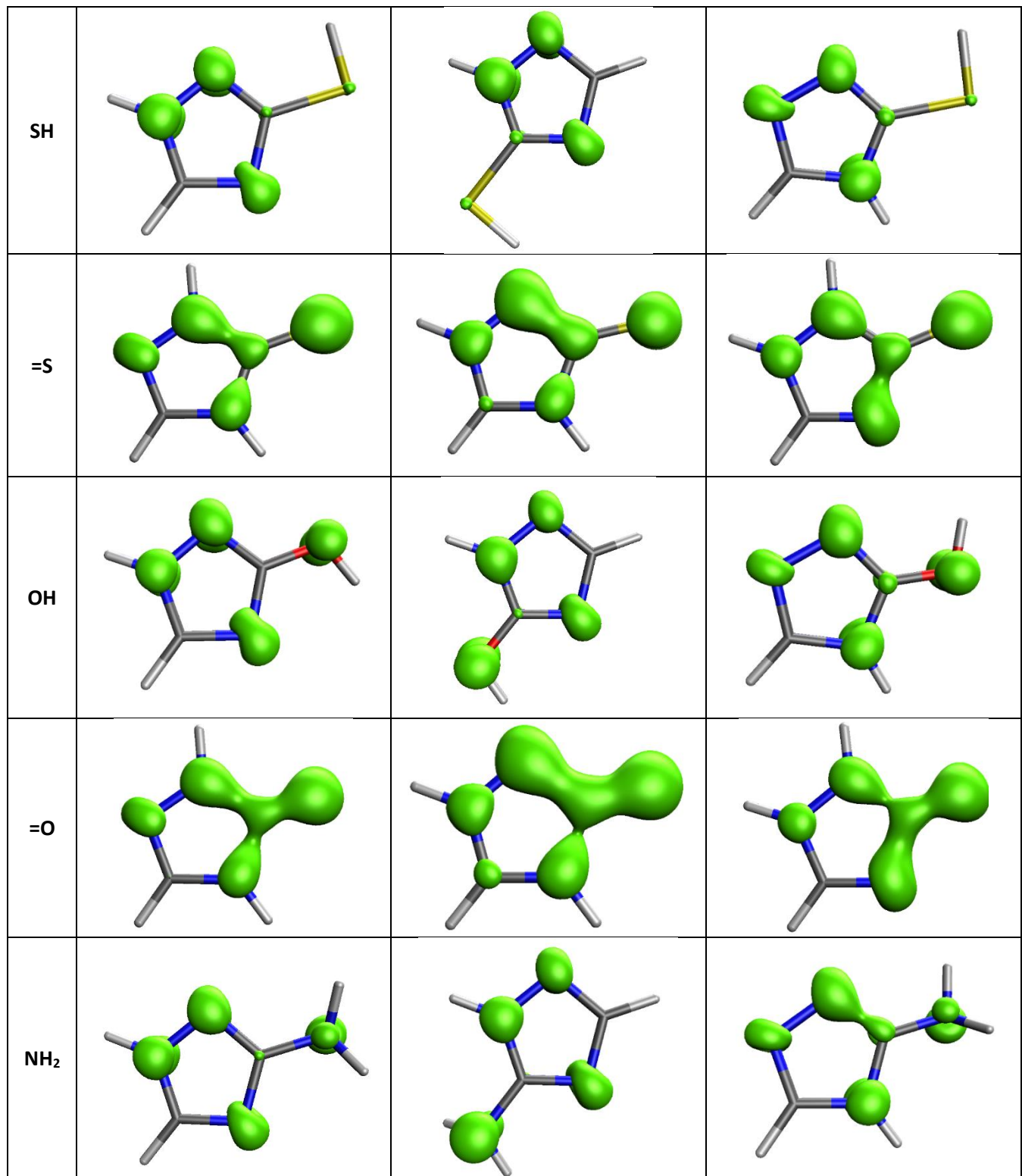












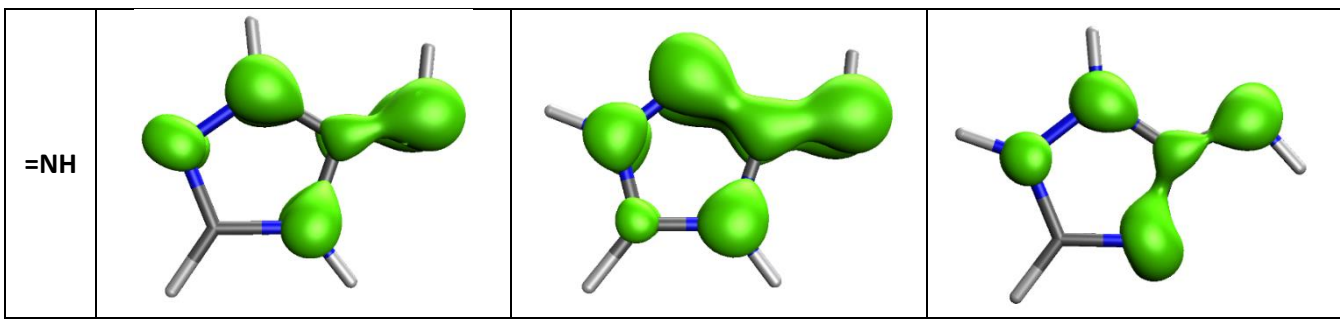
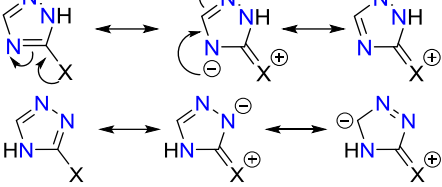
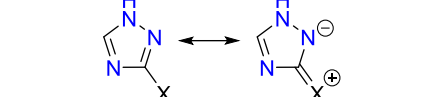
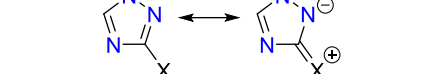
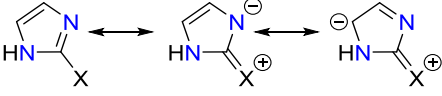
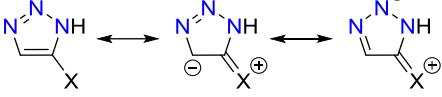
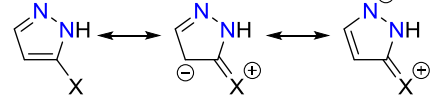
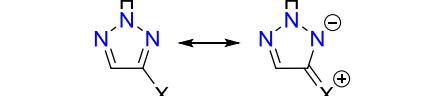
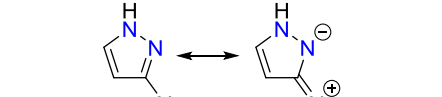
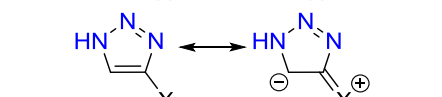
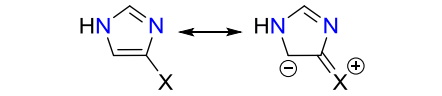
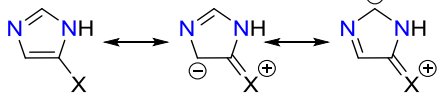
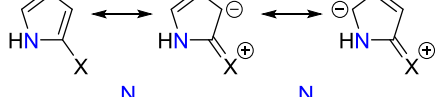
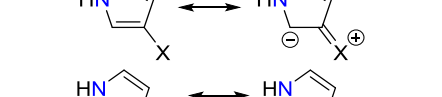
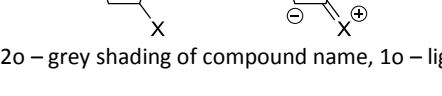


Table S5. Values of cSAR(X) for NO₂, Cl and NH₂ substituents, the number of inductive and resonance interactions between substituent and endocyclic N atoms in each heterocycle and resonance structures associated with resonance effect of substituents.

	indN ^a	resN ^b	indN_2 ^c	NO ₂	Cl	NH ₂	resonance (singly excited structures) ^d
1,2,4-triC5 (N1H)	2o	1o 1p	1	0.000	0.119	0.230	
1,2,4-triC3 (N4H)	2o	1o	1	-0.043	0.097	0.195	
1,2,4-triC3 (N1H)	2o	1o	1	-0.045	0.072	0.186	
imiC2	2o	1o	0	-0.056	0.079	0.182	
1,2,3-triC5 (N1H)	1o	1p	2	-0.101	0.033	0.135	
pyraC5	1o	1p	1	-0.112	0.024	0.126	
1,2,3-triC4 (N2H)	1o	1o	2	-0.118	0.003	0.115	
pyraC3	1o	1o	1	-0.128	-0.007	0.104	
1,2,3-triC4 (N1H)	1o	0	2	-0.140	-0.016	0.092	
imiC4	1o	0	1	-0.164	-0.034	0.079	
imiC5	1o	0	1	-0.164	-0.014	0.062	
pyrrC2	1o	0	0	-0.177	-0.018	0.058	
pyraC4	0	0	2	-0.224	-0.095	0.020	
pyrrC3	0	0	1	-0.216	-0.103	0.012	

^a indN – the number of endocyclic N atoms in *ortho* positions relative to substituent, 2o – grey shading of compound name, 1o – light grey shading, 0 – no shading.

^b resN – the number of endocyclic N atoms interacting via resonance (singly excited structures) with substituent and their position relative to substituent: o – *ortho*, p – *para*.

^c indN_2 – the number of non-*ortho* endocyclic N atoms interacting via induction with substituent.

^d electron-donating substituent delocalizes negative charge, electron-withdrawing positive; the structures look similar.

Table S6. Values of cSAR(X) of NO₂, Cl and NH₂ substituents in derivatives of selected six-membered heterocycles. Data taken from *Molecules* **2021**, *26* (21), 6543.

		NO ₂	Cl	NH ₂
triazine		0.043	0.124	0.292
pyrimidineC2		0.000	0.083	0.244
pyrimidineC4		-0.038	0.054	0.213
pyrazine		-0.065	0.031	0.181
pyridineC2		-0.078	0.016	0.163
pyridineC4		-0.097	-0.004	0.140
pyrimidineC5		-0.118	-0.020	0.113
pyridineC3		-0.128	-0.030	0.103

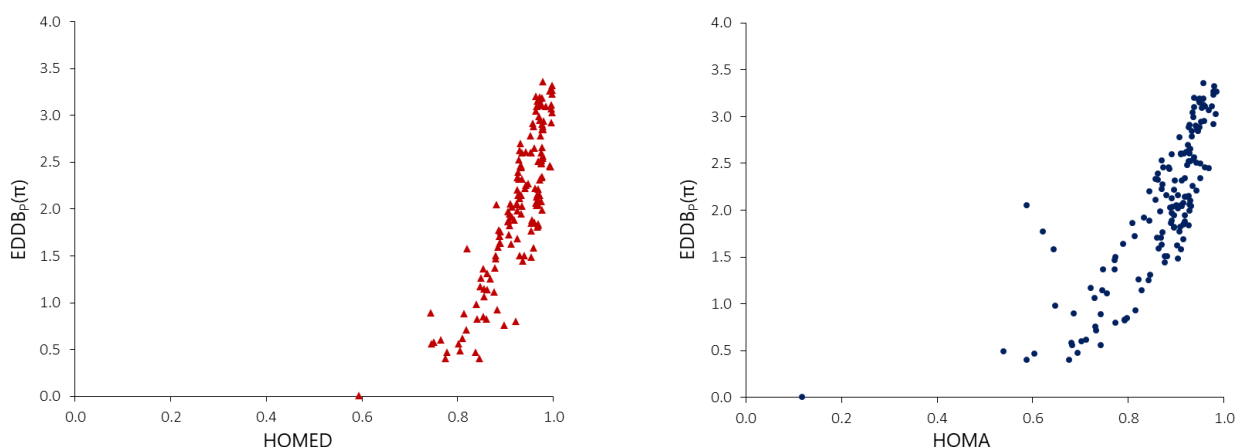
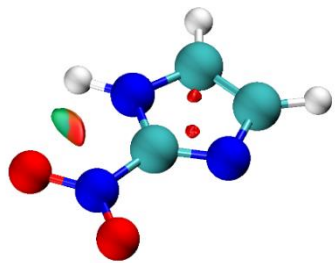
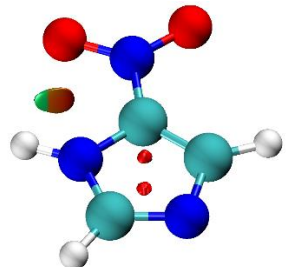


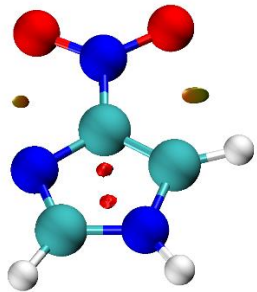
Figure S6. Relations between geometric aromaticity indices and the number of cyclically delocalized electrons from the EDDB_P(π) function.



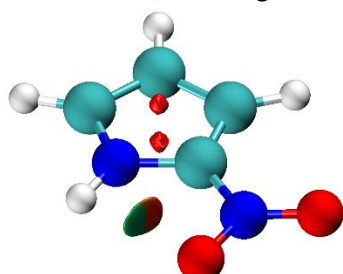
imiC2-NO2
2.410 Å, 91.9 deg



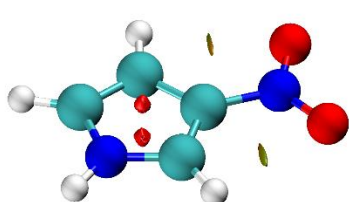
imiC5-NO2
2.461 Å, 91.01 deg



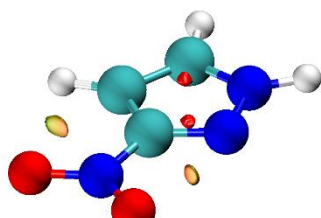
imiC4-NO2



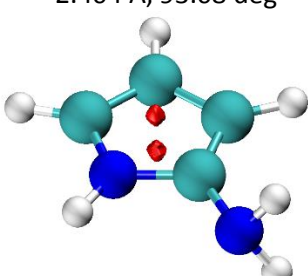
pyrrC2-NO2
2.404 Å, 93.08 deg



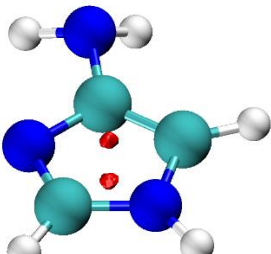
pyrrC3-NO2



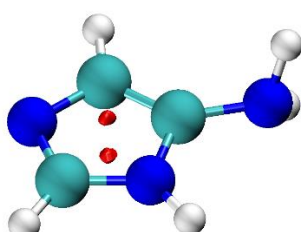
pyraC3-NO2



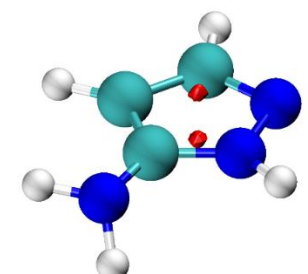
pyrrC2-NH2
2.623 Å, 65.93 deg



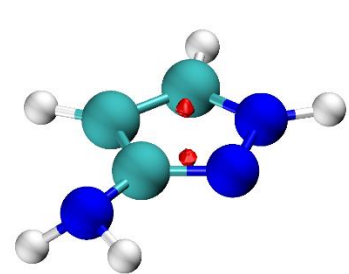
imiC4-NH2
2.474 Å, 73.95 deg



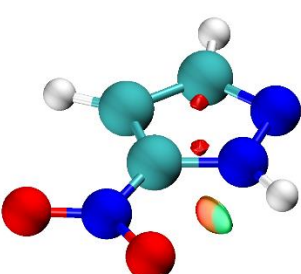
imiC5-NH2
2.674 Å, 64.21 deg



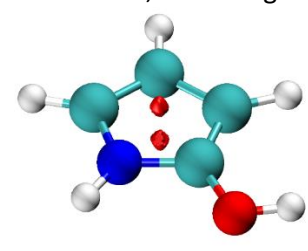
pyraC5-NH2
2.700 Å, 61.72 deg



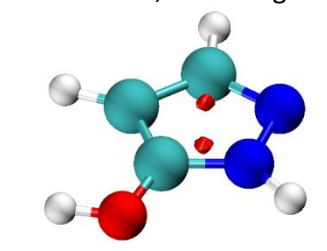
pyraC3-NH2
2.467 Å, 72.56 deg



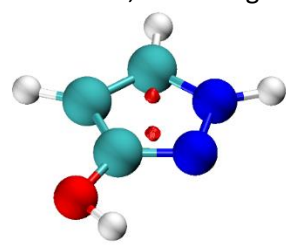
pyraC5-NO2
2.481 Å, 89.44 deg



pyrrC2-OH
2.575 Å, 64.33 deg



pyraC5-OH
2.625 Å, 61.49 deg



pyraC3-OH
2.338 Å, 78.02 deg

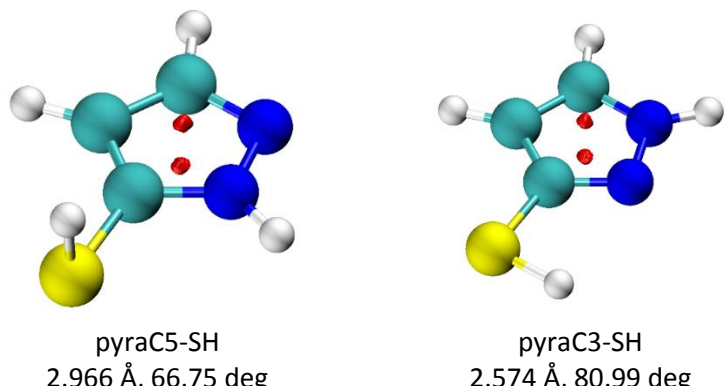


Figure S7. Non covalent interaction analysis (NCI method). Reduced density gradient isosurfaces ($\text{RDG} = 0.5$), colored according to the value of $\text{sgn}(\lambda_2(r)) \cdot \rho(r)$. Distances and angles of $\text{DH} \cdots \text{A}$ *ortho* contacts ($\text{D} = \text{N}, \text{O}, \text{S}; \text{A} = \text{N}, \text{O}$).

Table S7. Keto, thioketo and imino forms of studied 5-membered heterocycles with their $\text{EDDB}_P(\pi)$, $\text{cSAR}(X)$, HOMED, CX bond lengths (d_{CX}) and ΔE values (in kcal/mol).

	cyclic π -electron delocalization									
$\text{EDDB}_P(\pi)$	2.050	1.581	1.365	0.896	0.713	0.605	0.564	0.491	0.474	0.471
HOMED	0.881	0.820	0.853	0.744	0.818	0.764	0.745	0.805	0.778	0.838
$\text{cSAR}(X)$	-0.416	-0.322	-0.272	-0.306	-0.165	-0.183	-0.221	-0.237	-0.167	-0.223
$d_{CX}/\text{\AA}$	1.241	1.223	1.223	1.228	1.214	1.218	1.215	1.223	1.210	1.220
ΔE^a	33.8	45.6	15.9	7.7	-6.8	-9.0	15.6	12.5	13.5	15.9
	thioketo forms (=S)									
$\text{EDDB}_P(\pi)$	2.225	2.203	2.222	1.310	0.930	0.831	0.853	0.762	0.825	0.803
HOMED	0.961	0.924	0.940	0.862	0.882	0.840	0.854	0.897	0.860	0.921
$\text{cSAR}(X)$	-0.564	-0.450	-0.389	-0.444	-0.253	-0.283	-0.333	-0.340	-0.256	-0.316
$d_{CX}/\text{\AA}$	1.698	1.673	1.668	1.679	1.653	1.662	1.662	1.666	1.650	1.660
ΔE^b	35.3	38.8	9.7	11.1	-6.6	-8.3	14.7	14.0	16.2	17.1
	imino forms (=NH)									
$\text{EDDB}_P(\pi)$	1.775	0.982	1.113	0.889	0.619	0.583	0.562	0.011	0.403	0.406
HOMED	0.886	0.838	0.877	0.813	0.810	0.749	0.802	0.593	0.773	0.845
$\text{cSAR}(X)$	-0.391	-0.279	-0.241	-0.281	-0.130	-0.150	-0.197	-0.135	-0.137	-0.188
$d_{CX}/\text{\AA}$	1.309	1.293	1.291	1.298	1.281	1.285	1.285	1.281	1.277	1.288
ΔE^c	55.7	65.0	36.6	30.9	13.4	11.0	34.7	22.9	30.4	34.0

a – the energy of keto form relative to the enol form; b – the energy of thioketo form relative to the thiol form;
c – the energy of imino form relative to the amino form.

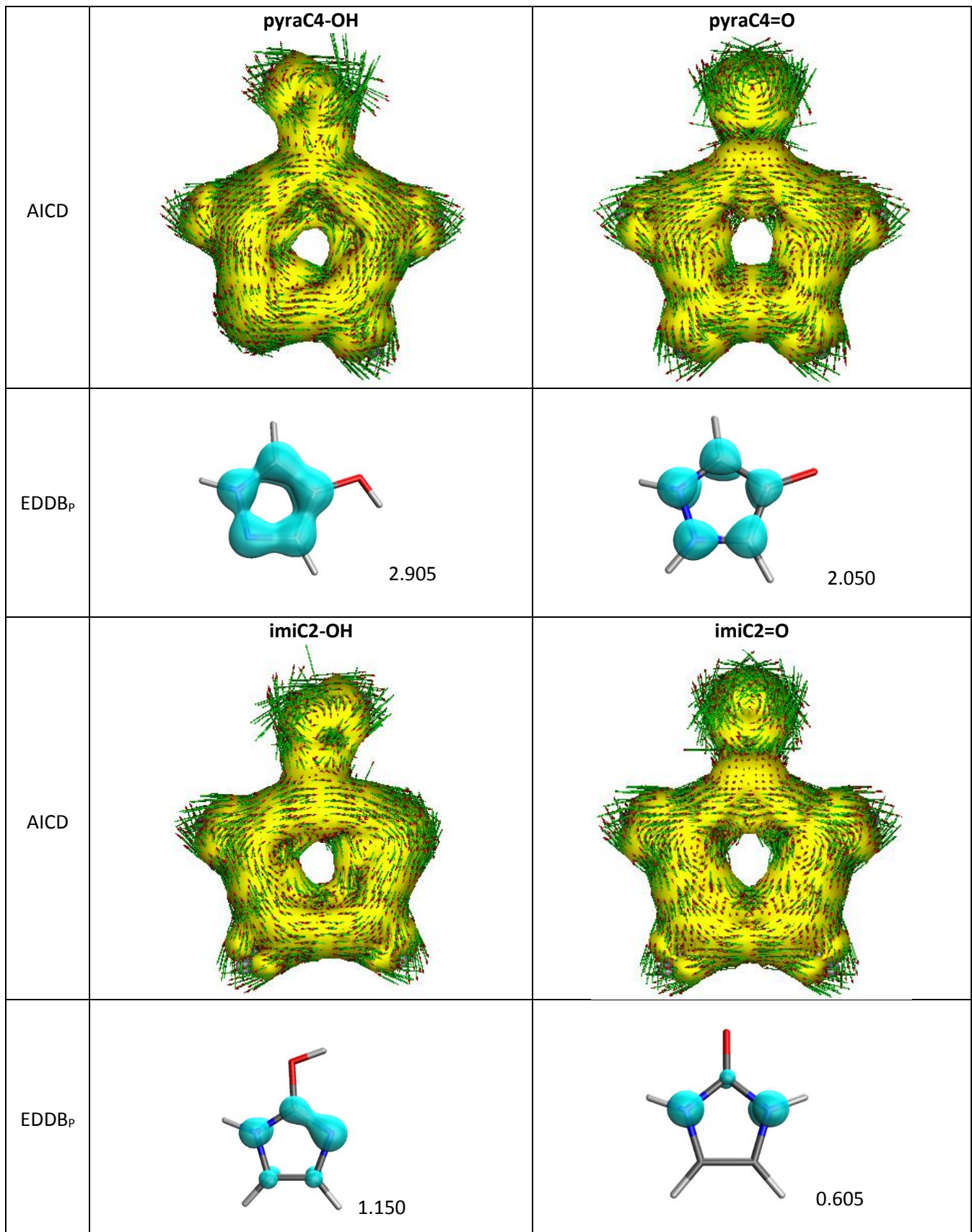


Figure S8. Anisotropy of the induced current density (AICD) plots (isosurface=0.03) and EDDB_P isosurfaces (0.02) with corresponding populations of cyclically delocalized electrons for enol and keto forms of substituted imidazole and pyrazole.

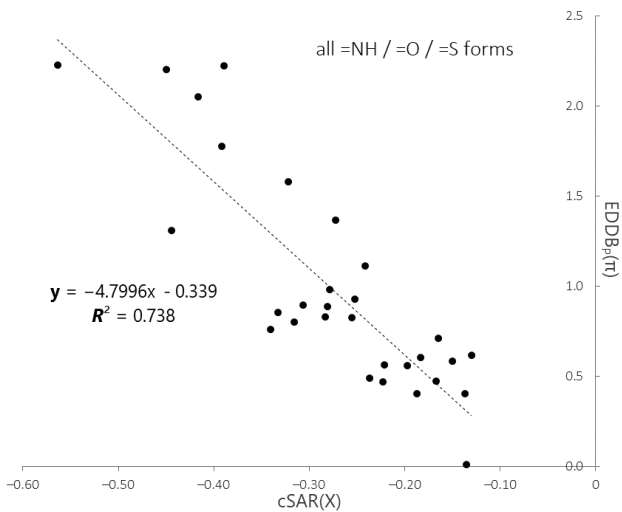
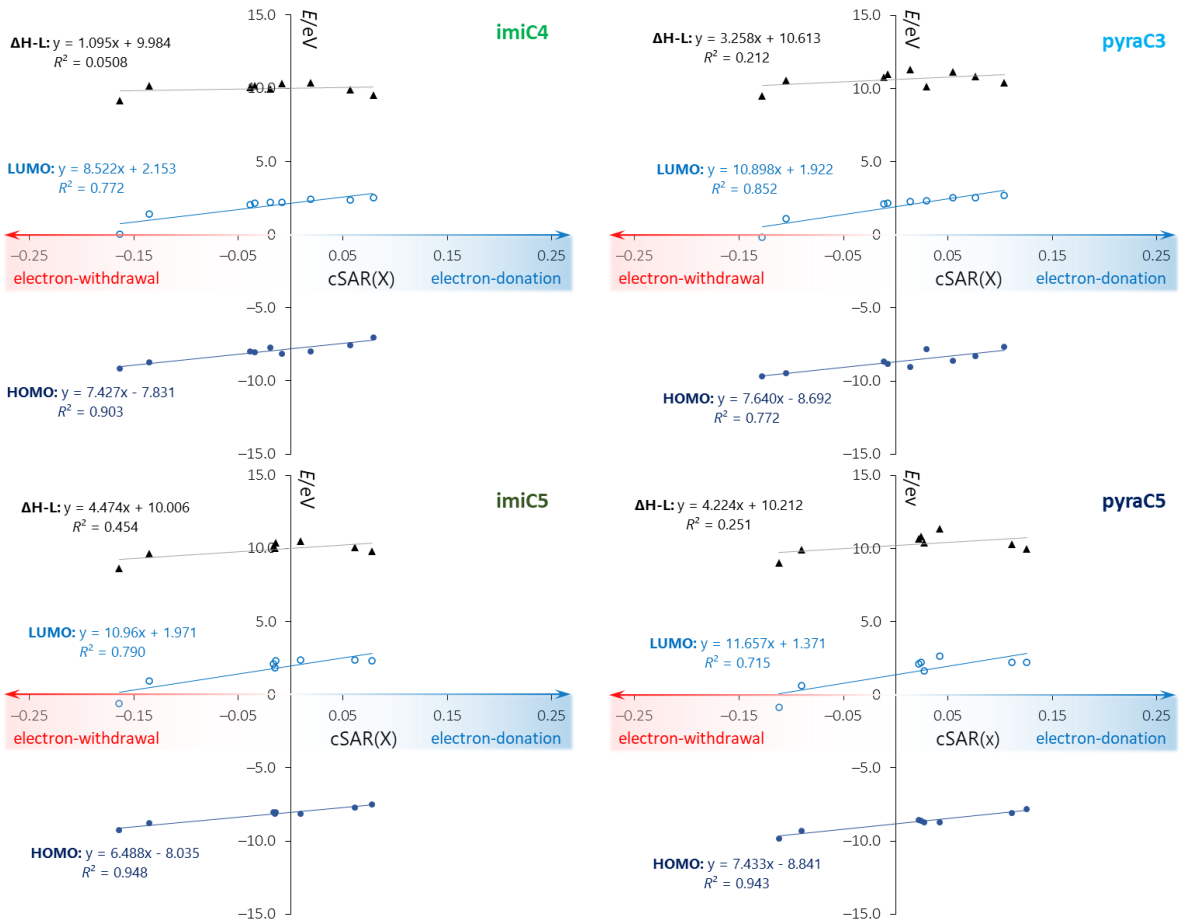
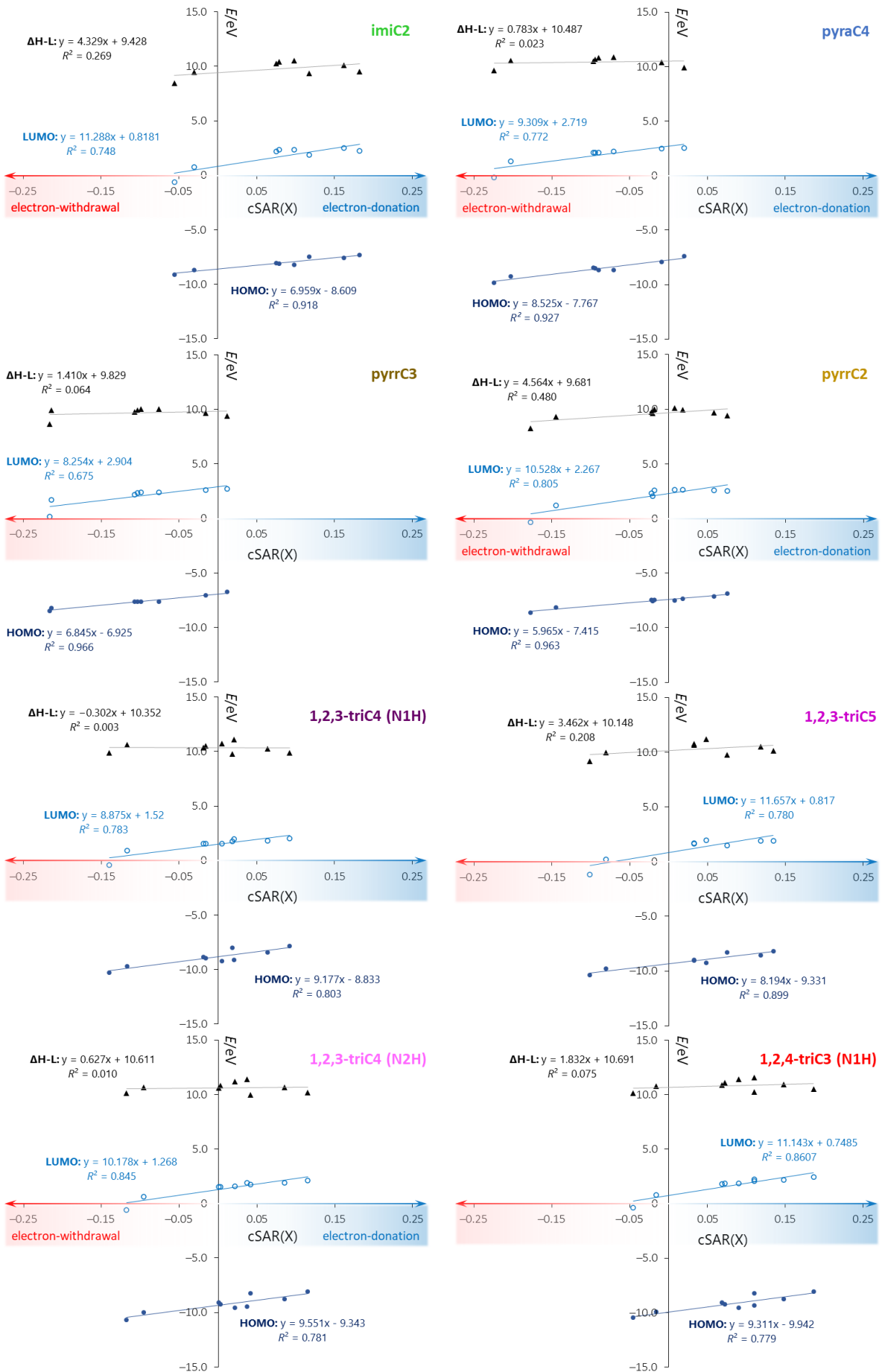


Figure S9. Correlation between the number of cyclically delocalized electrons and electron withdrawing properties of =NH/=O/=S groups for all studied heterocycles.





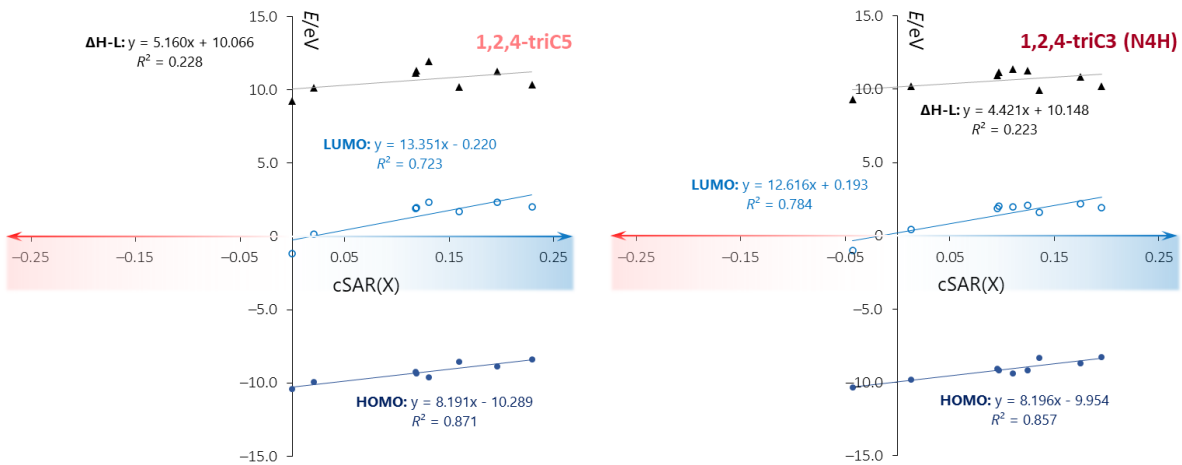


Table S8. Summary of slopes from Figure S9.

	HOMO	LUMO
1,2,4-triC3(N1H)	9.311	11.143
1,2,3-triC4(N1H)	9.177	8.875
pyraC4	8.525	9.309
1,2,3-triC4(N2H)	8.466	6.861
1,2,3-triC5(N1H)	8.194	11.657
1,2,4-triC5(N1H)	8.191	13.351
1,2,4-triC3(N4H)	8.034	7.678
pyraC3	7.640	10.898
imiC4	7.427	8.522
pyrrC3	6.844	8.254
imiC5	6.488	10.962
pyrrC2	5.965	10.528
pyraC5	5.951	4.627
imiC2	5.495	11.288

Table S9. Reference bonds lengths (Å) calculated at revDSD–PBE/PBEP86–G3BJ/def2–TZVPP level of theory and values of HOMED normalization constants α .

HOMED	d_s	d_d	d_o	α
CC	1.5266 ethane	1.3312 ethene	1.3936 benzene	82.226
CN	1.4643 methylamine	1.2709 methylimine	1.3337 triazine	84.611
NN	1.4687 	1.2399 	1.3175 	62.022

Table S10. AICD plots (isosurface = 0.03) of selected substituted and unsubstituted systems.

